POLITECNICO DI MILANO

Facoltà di Ingegneria dei Sistemi
Corso di Laurea in Ingegneria Biomedica

Automatic classifier of stereoelectroencephalographic signals for epileptogenic zone localization in drug-resistant epilepsy

Relatore:
Prof. Giancarlo FERRIGNO

Correlatore:
Ing. Elena DE MOMI

Tesi di Laurea di:
Luca Fontana, matricola 782034

Anno Accademico 2012-2013

Automatic classifier of stereoelectroencephalographic signals for epileptogenic zone localization in drug-resistant epilepsy

Abstract

Epilepsy is a disabling neurological condition and it's a relevant risk of death factor. Its main manifestation is the seizure which can present a wide range of symptoms, from convulsion to unconsciousness. Epilepsy is usually classified in two main subtypes: generalized, if the seizure triggering neuronal population is non clearly identifiable, partial when the epileptogenic cortex is very confined. Focal epilepsies are drug resistant in the 30-40% of the times and the only available treatment is the cortical ablation surgery in order to remove the seizure triggering cortex. The pre-operative planning stage is extremly critical because the surgery is aimed at removing only the epileptogenic area without any damage to the healty surrounding zone, so as leading the patients to a total seizure free condition with the least neurological damage.

Localizing the epileptogenic zone (EZ) is a quite complex task, performed by neurologists, who have to analyze a huge amount and variety of data (patient's clinical history and symptoms, CT and MRI images, encefalographic signals). Sometimes, when the EZ localizalization can't be accomplished with non-invasive techniques, surgeons proceed with the insertion of electrodes within the most probable epileptogenic brain areas (according to neurologists), in order to record the neuronal activity with high spatial and temporal resolution.

The objective of this project was the implementation and the validation of an automatic classifier able to recognise leads implanted in an epileptogenic zone from the ones inserted within a healty brain region. In order to obtain a total healing of the epileptic subject the complete ablation of the seizure triggering cortex is required, making mandatory the absolute absence of False Negatives in the classification performance.

A non-linear non-parametric correlation measure was computed

for each couple of channels of the StereoElectroencephalography (SEEG), a depth-EEG recording method, in order to estimate connectivity matrixes, which are the representation of how much each channel (leads of the electrodes) is mutual dependant from the others. Connectivity matrixes were used as input for reconstruct the functional networks of the interaction between the neuronal population corresponding to the SEEG leads, shifting the problem in the graph theory domain, considering each matrix the representation of the inward and outward connections of a network.

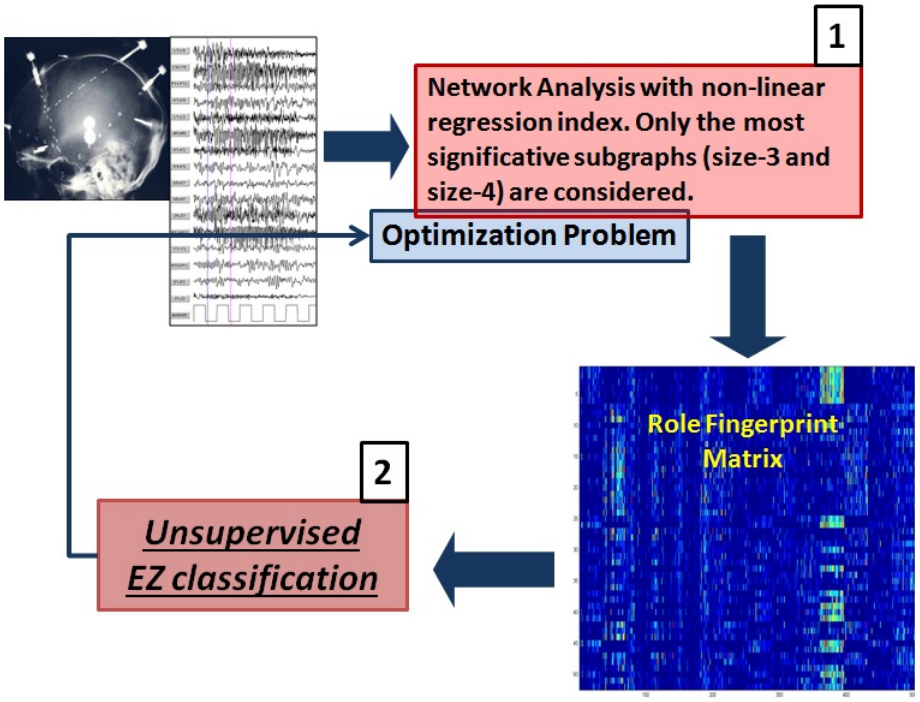

Figure 1: 1. From the estimated connectivity matrixes, the corresponding networks are reconstructed. Only the most significative subgraphs of 3 and 4 nodes are used to characterize SEEG leads. 2. Clustering and classification of SEEG leads, on the base of the features extracted in the previous stage. Results were optimized on a subset of the dataset.

The implemented classification algorithm, starting from the reconstructed networks, is made by two main stages:

1. A deep network analysis is performed. First of all size-3 and size-4 subgraphs are enumerated from the reconstructed networks, then they are collected in classes and then only the most statistical significative are selected. The statistical significance is computed comparing the subgraph occurrence to the one in a random network model. Then the most significative subgraphs become the starting point for the *Roles Fingerprint Matrix,* assigning to each node a set of values, called *roles*, computed taking into account its inward and outward connections and the subgraphs where it occurs (stage 1 in Figure 1).

2. The Roles Fingerprint Matrix is the input of two unsupervised clustering methods, K-Means and Affinity Propagation. Classification is performed with the apriori knowledge of one EZ leads, which is used to find the EZ cluster. Each lead assigned to EZ cluster is considered as Positive (EZ), while leads assigned to each other cluster are considered Negative (NEZ). The algorithm was optimized considering a subset of patients. The main optimization constraint is the minimizing the number of False Negative. The, in the False Negative minimum domain, also the False Positive is minimized. Finally also leads of the remaining patiens were classified and classification performance was evaluated (stage 2 in Figure 1).

In this project 18 clinical cases were considered, drug-resistant partial epilepsy (in particular Focal Cortical Dysplasia, Post Traumatic epilepsy, Polymicrogyria) and seizure free after the cortex ablation surgery.

Each patient was implanted with a variable number (from 5 to 15) of multileads electrodes. The dataset was made by 3 minutes of multichannel interictal SEEG signal. Each contact has recorded the surrounding electrical neuronal activity for several weeks. An expert neurologist has selected an interictal signal window 3 minutes long,

labeling each channel as epileptogenic (EZ) or non-epileptogenic (NEZ).

The difference between K-Means and Affinity Propagation clustering was checked with a Chi-Square test.

Results were analyzed both all together and separately in two groups. One group was made by the patients affected by Focal Cortical Dysplasia, the other by patients with Post Traumatic epilepsy and Polymicrogyria. The reason of this choice is that the epileptogenic zone in Focal Cortical Dysplasia is usually more well-defined, and so easier to be localized, than the one in the other two types of epilepsies.

The obtained classifier has a quite low False Negative Rate and also a reasonable number of False Positive, especially in patients with Focal Cortical Dysplasia. Instead, talking about the other cases, the False Negative number is unacceptable, considering the objective of the work. However, since the dataset is really poor, especially for the number of non-Focal Cortical Dysplasia cases, it's impossible to definitively draw some conclusions.

This work it's just a starting point. Future improvements could include a deeper network analysis, considering also size-k subgraphs with $k \geq 5$, paying attention to the script implementation, which must have a very parallelized structure. Plus a very powered-up hardware is required. Another possible upgrade could be the use of bayesian method or multivariate variance analysis on the Roles Fingerprint Matrix. Finally, in order to provide a software suited for a clinical use, a very user-friendly GUI could be designed, able to give out also information about the morphology of the patients' brain, fusing the information about the epileptogenicity to the information contained in the CT and MRI images.

Key-Words: epilepsy, classification, automatic, intericatal, stereoelectroencefalography, leads.

Sommario

L'epilessia è una patologia neurologica altamente debilitante e costituisce un serio pericolo per la vita di chi ne è affetto. Si manifesta attraverso crisi che possono presentare molti tipi diversi di sintomi, dalle convulsioni alla perdita di conoscenza. Essa è classificata generalmente in due sottotipi: generalizzata se la popolazione neuronale che genera l'attacco non è identificabile, parziale se invece la corteccia epileptogenica è limitata e definita. Le epilessie focali sono nel 30-40% dei casi refrattarie a trattamenti farmacologici e l'unica terapia possibile diventa l'ablazione chirurgica della parte di corteccia cerebrale che dà origine alla crisi. La fase di pianificazione preoperatoria diventa estremamente critica poichè l'operazione mira a rimuovere solamente la parte di cervello malata cercando di non danneggiare le sezioni circostanti, in modo da portare il soggetto alla guarigione totale dalle crisi, introducendo il minor danno neurologico possibile.

L'individuazione della zona epileptogenica (EZ) è un'attività molto complessa deputata ai neurologi, i quali devono analizzare un gran quantità e varietà di dati (storia clinica e sintomi del paziente, immagini CT e MRI, segnali encefalografici). In particolare, quando la localizzazione del focolaio epileptogeno risulta troppo complessa, si ricorre all'uso di una tecnica invasiva che consiste nell'inserimento di elettrodi all'interno della corteccia cerebrale con lo scopo di registrare l'attività neuronale con alta risoluzione spaziale e temporale nelle zone dove il neurologo ritiene possa esserci più probabilmente la zona epileptogenica. In questo progetto sono stati presi in considerazione segnali ottenuti con la tecnica della Stereoelettroencefalografia.

Lo scopo di questo progetto di tesi è implementare e validare un classificatore automatico in grado di discernere contatti impiantati in una zona epileptogenica da quelli che si trovano a contatto con

corteccia cerebrale normale, utilizzando il segnale sopra descritto. La priorità deve essere data all'ottenimento di un numero di falsi negativi (contatti epileptogenici classificati come sani) il più basso possibile, perchè per avere la completa guarigione del soggetto epilettico è indispensabile la totale rimozione della corteccia epileptogena.

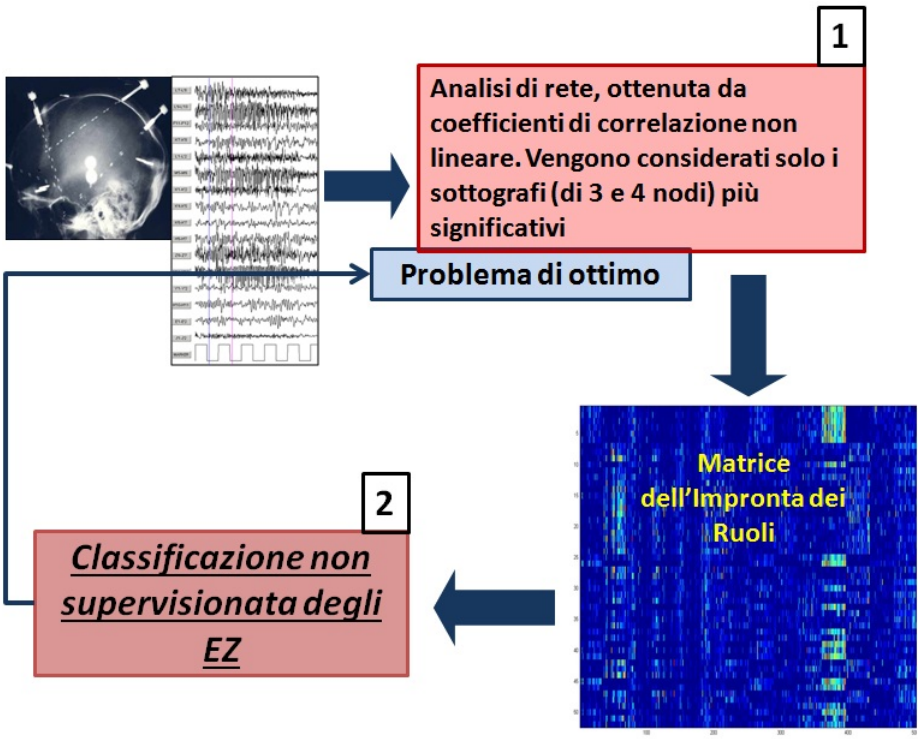

Figure 2: 1. Dalle matrici di connettività stimate dal segnale SEEG, sono state ricostruiti i corrispondenti circuiti di rete. All'interno di esse sono stati indivduati i sottografi più significativi di 3 e 4 nodi e sono stati usati per caratterizzare i contatti SEEG. 2. I contatti dell'SEEG sono stati clsuterizzati e classificati sulla base dei parametri estratti al punto 1. I risultati sono stati ottimizzati su un sottoinsieme del dataset.

Dai segnali SEEG sono state calcolate delle matrici di connettività, utilizzando una misura di correlazione non lineare e non parametrica per ogni coppia di contatti. Le matrici contengono l'informazione di quanto ogni coppia di canali (contatti degli elet-

trodi) è mutualmente dipendente. Dalle matrici di connettività, basandosi sulla teoria dei grafi, sono state ricostruite le reti funzionali di interazione fra le zone neuronali corrispondenti ai contatti della SEEG. Ogni matrice è la rappresentazione delle connessioni di ingresso e di uscita dei vertici di un grafo.

L'algoritmo di classificazione utilizza le ricostruzioni delle reti come input ed è costituito da due passaggi principali:

1. E' stata effettuata un'approfondita analisi di rete che prevede prima l'enumerazione di tutti i sottografi di 3 e 4 nodi, la loro relativa suddivisione in classi e la scelta di quelli statisticamente più significativi, utilizzando un confronto con un modello di rete casuale. I sottografi statisticamente più significativi sono stati utilizzati per la generazione della *Matrice dell'Impronta dei Ruoli* assegnando ad ogni nodo una serie di valori, chiamati *ruoli,* sulla base delle sue connessioni di ingresso e di uscita all'interno di un determinato sottografo (blocco 1 nella figura 2).

2. La Matrice dell'Impronta dei Ruoli è stata poi utilizzata come dataset per due algoritmi di clustering, K-Means e Affinity Propagation. La classificazione è stata effettuata utilizzando come conoscenza a priori un singolo contatto etichettato come EZ (epileptogenico) in modo da individuare il cluster EZ. Tutti i contatti contenuti nel cluster EZ sono stati classificati come positivi, mentre i contatti contenuti in tutti gli altri clusters sono stati considerati negativi. L'algoritmo è stato ottimizzato su un sottoinsieme dei pazienti costituenti il dataset minimizzando prima i falsi negativi e poi, nel dominio così trovato, i falsi positivi. Infine sono stati classificati i contatti dei restanti quattordici pazienti e sono state valutate le performance del classificatore (blocco 2 nella figura 2).

In questo lavoro sono stati presi in considerazione 18 casi clinici,

tutti affetti da epilessia parziale farmaco resistente (in particolare affetti da Displasia Corticale Focale, epilessia Post Traumatica e Polimicrogiria) e guariti totalmente dalle crisi dopo l'intervento di resezione della corteccia. I dati utilizzati consistevano in 3 minuti di segnale interictale encefalografico registrato con la tecnica invasiva della Stereoelettroencefalografia. Ogni paziente ha subito l'impianto di un numero variabile (da 5 a 15) di elettrodi multicontatto. Ogni contatto ha registrato per alcune settimane l'attività elettrica delle popolazione neuronali lui adiacenti. Un neurologo esperto ha selezionato 3 minuti di segnale interictale di ogni paziente, catalogando ogni canale in epileptogenico, o non epileptogenico.

Per verificare la diversistà fra K-Means e Affinity Propagation è stato effettuato il test del chi-quadro. I risultati ottenuti sono stati valutati sia nella loro totalità sia analizzando semparatamente i casi di epilessia dovuta a Displasia Corticale Focale da quelli dovuti a Post Traumatica e Polimicrogiria. La divisione è stata fatta poichè l'individuazione della zona epileptogenica è generalmente molto più semplice per le patologie dovute a Displasia Corticale.

Il classificatore ottenuto riesce a classificare piuttosto bene e con un ragionevole numero di falsi positivi i contatti EZ nei casi di epilessia dovuti a Displasia Corticale. Negli altri casi presenta invece un alto numero di falsi negativi, inaccettabili per l'obiettivo preposto. Tuttavia, essendo il dataset piuttosto limitato, soprattutto per quel che riguarda le epilessie non dovute a Displasia Corticale, non è possibile trarre delle conclusioni definitive. L'algoritmo andrebbe provato su un più ampio dataset, spostando l'attenzione anche su altre finestre del segnale SEEG (onset, ictale, post-ictale).

Eventuali sviluppi futuri prevedono una più approfondita analisi di rete, in particolare estendendo la ricerca a sottografi di dimensioni maggiori (5 nodi o più), anche se questo particolare ampliamento del metodo richiede la riscrittura di alcuni script in modo da

renderli più performanti e una struttura hardware particolarmente avanzata. Un altro possibile ampliamento riguarda l'analisi della matrice dell'impronta dei ruoli, che può essere elaborata utilizzando reti bayesiane o analisi multivariate di varianza. Infine, in previsione di un uso clinico, si potrebbe implementare un'interfaccia grafica, in grado non solo di fornire informazioni sull'epileptogenicità delle varie zone in analisi, ma anche sulla posizione dei contatti e sulla morfologia del cervello in esame, fondendo anche informazioni derivanti dalle immagini CT e MRI di ogni paziente.

Parole chiave: epilessia, classificazione, automatica, stereoelettroencefalografia, contatti.

Ringraziamenti

Desidero ringraziare il Prof. Giancarlo Ferrigno e l'Ing. Elena De Momi per le indicazioni, i consigli e le revisioni apportate a questo lavoro di tesi.

Un grosso ringraziamento anche alla Dott.sa Giulia Varotto ed all'Ing. Ferruccio Panzica, che mi hanno aiutato a comprendere molti aspetti critici riguardanti questo lavoro di tesi.

Inoltre vorrei ringraziare la Dott.sa Laura Tassi per i dati forniti, per le spiegazioni del problema clinico e per avermi incoraggiato fin dall'inizio.

A great thanksgiving to Yohannes Kassahun, Elmar Berghofer, for their help and explanation about the computer science.

Vorrei poi ringraziare la mia famiglia, che mi ha fornito costante supporto, e mi ha sopportato durante questi mesi.

Infine, non ultimi per importanza, ringrazio i miei amici e tutte le persone che ho conosciuto in questi mesi, compagni di tesi e non, che mi hanno supportato ed accompagnato per tutto il lavoro.

Contents

List of Figures

List of Tables

Chapter 1

Introduction

1.1 Epilepsy

Epilepsy is a neurological chronic condition that affects about 1% of the population. It is characterized by recurrent and unprovoked seizures, which are the main manifestation of this disease. A seizure is defined as a paroxysmal, self-limited change in behaviour associated with excessive electrical discharge from the central nervous system. Epilepsy is defined as a condition of recurrent seizures and medical intractable recurrent seizures despite optimal treatment under the direction of an experienced neurologist over a two to three year period. Seizures have been classified based upon their clinical manifestations which had some relevance for patients and physicians but was of limited diagnostic or prognostic value. This classification scheme is based entirely on the distinct behavioural and electrophysiologic features of the seizures themselves. According to this classification, an epileptic disorder is defined as either being *generalized*, *partial (focal)* or *undetermined*. Primary *generalized* seizures start as a disturbance in both hemispheres synchronously without evidence of a localized onset zone. The manifestations of these seizures tend to be major motor seizures of a tonic, clonic, tonic-clonic, my-

oclonic or atonic type. They also include minor events of the petit mal (absence) type. *Partial forms* of epilepsy start in a focal area of the brain and may remain localized without alteration of consciousness. These events are referred to as simple partial seizures and the symptoms vary with the area of the brain affected. If the event spreads and alters consciousness it is referred to as a complex partial seizure. If the event spreads further and leads to a major motor seizure it is referred to as a secondarily generalized seizure and may be quite difficult to distinguish from the primary generalized forms. Partial seizures often arise from the limbic structures of the temporal and frontal lobes but can occur from any cortical region and are often quite refractory to medical therapy alone. In general , patients with partial seizure disorders are the most amenable to surgical intervention [6]. Due to the described symptoms, epilepsy is considered a disabling disorder. Furthermore people with epilepsy are at risk for death because of four main problems :

- Status Epilepticus is a life-threatening condition in which the brain is in a state of persistent seizure. Traditionally it is defined as one continuous, unremitting seizure lasting longer than 5 minutes, or recurrent seizures without regaining consciousness between seizures for greater than 5 minutes [7]. It is always considered a medical emergency. There is some evidence that five minutes is sufficient to damage neurons and that seizures are unlikely to self-terminate by that time.

- Trauma from seizure, due to strong convulsions [8].

- Sudden Unexpected Death in Epilepsy (SUDEP) is term used when a person with epilepsy suddenly dies, and the reason for the death results from unexplained respiratory failure or cardiac arrest after seizures (this should not be confused with status epilepticus). Post mortem examination usually reveals no

abnormalities in victims [9].

- Suicide associated with depression, because subject affected by epilepsy cannot often live a normal life [8].

From the point of view of the electrophysiology (recorded on or within the scalp), it is important the evolution in time of a seizure. In an epileptic subject's electrophysiological signals, may be identified four major temporal phases of the seizure [10]:

1. *Preictal phase*, is the temporal window just before the real seizure. It can last from minutes to days and makes the subject acts and feels differently, even if not everyone experiences something at this stage. Preictal activity often present spikes with high power. At the end of this stage, electrical signal is usually affected by high frequency ripples, which mark the seizure *onset*.

2. *Ictal phase*, is the stage when the actual seizure develops. During this time there will be an electrical storm in the subject brain, making him present cardiovascular, metabolic and electrophysiological changes.

3. *Post Ictal*, takes place after the real seizure and it's a neuronal reovery stage. During this stage the most involved brain areas are often reftactory, showing a very little electrical activity.

4. *Interictal phase* is the time between seizure. Anyway a lot of epileptic subjects show some kind of symptoms also during this stage.

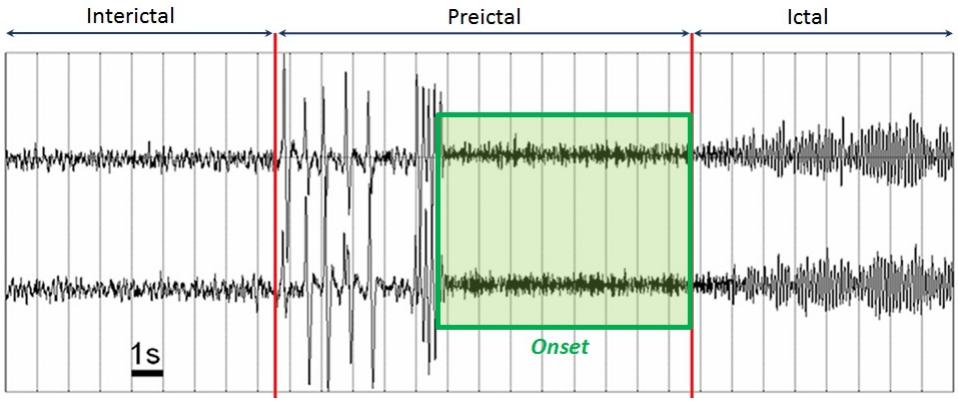

Figure 1.1: Example of three different phases of the SEEG in an epileptic subject. Interictal phase doesn't show any anomaly. Preictal shows some fast transient events, which disappears in the onset. Ictal phase shows high amplitude waves.

As told above, under the term "*epilepsy*" may be found a large number of different pathologies. In the following will be described epilepsy type considered in this work. They are very different from each other, both for the etiology and symptomps. Their only common aspect is that they are classified as partial epilepsies.

1. *Focal Cortical Dysplasias (FCD).* They are part of an array of disorders described variously as disorders of cortical development, cortical dysplasias, cortical dysgenesis, or neuronal migration disorders. This kind of epilepsy was studied for the first time by Taylor in 1971 [11]. In fact this group of pathology is also known as Taylor Type Epilepsy. Classification of these disorders depends on either their pathological characateristics or the proposed origin of the pathological elements. Especially in 2004 [12] a general classification have been proposed and FCD epilepsies have been splitted in 2 macro groups: (a) Type I: FCD cases with non evidence of abnormal cells. (b) Type II: FCD epilepsies which presents dysmorphic cells and/or balloon cellsFocal cortical dysplasia is a significant cause of medically

refractory epilepsy [13]. During the last 45 years, developments in imaging, electroencephalography, and electrocorticography have allowed more patients with medically refractory epilepsy to undergo resective surgery. In this thesis have been considered 15 patients with FCD type II

2. *Polymicrogyria (PMG).* Developmental malformation of the human brain characterized by an excessive number of small convolutions (gyri) on the surface of the brain, resulting in structurally abnormal cerebral hemispheres. Either the whole surface (generalized) or parts of the surface (focal) can be affected. Children born with it may suffer from a wide spectrum of other problems, including: global developmental disabilities, mild to severe mental retardation, motor dysfunctions including speech and swallowing problems, respiratory problems, and seizures. Only two patients affected by PMG have been considered in this work [14].

3. *Post Traumatic Epilepsy (PTE).* Form of epilepsy that results from brain damage caused by physical trauma to the brain (traumatic brain injury, abbreviated TBI). A person with PTE suffers repeated post-traumatic seizures (PTS, seizures that result from TBI) more than a week after the initial injury [15]. PTE is estimated to constitute 5% of all cases of epilepsy and over 20% of cases of symptomatic epilepsy (in which seizures are caused by an identifiable organic brain condition). It is not known how to predict who will develop epilepsy after TBI and who will not. However, the likelihood that a person will develop PTE is influenced by the severity and type of injury; for example penetrating injuries and those that involve bleeding within the brain confer a higher risk. The onset of PTE can occur within a short time of the physical trauma that causes it, or months or years after. People with head trauma may remain

at a higher risk for seizures than the general population even decades after the injury. Diagnostic measures include electroencephalography and brain imaging techniques such as magnetic resonance imaging, but these are not totally reliable [16].

The mainstay of treatment of epilepsy is anticonvulsant and barbituric medications, but 30% of the patients cannot control seizures with a mix of three different drugs. For drugs resistant epilepsy the option is a cortical ablation surgery. The requirement for this treatment is a very localized onset brain area and the goal is the total seizures control, although sometimes anticonvulsant medications may still be required, especially when the epileptogenic cortex isn't totally removed. This situation occurs when some cortical regions, identified as epileptogenic, are involved in too critical neurologic functions (eloquent cortex) or when the epileptogenic zone isn't correctly detected.

Detecting the onset region, also called Epileptogenic Zone (EZ) is a very difficult task, which takes long time and a large number of clinical exams, which must be interpreted by neurologists with a deep visual inspection. Usually clinicians, in order to make an accurate diagnosis, proceed first with a detailed study of the patient's clinical history, analyzing symptomps, neurological condition and the family clinical history. Then they analyze different types of images, including CT, MRI, SPECT, PET in order to identify any anatomical malformations or functional anomalies. At the same time the patient is video-recorded during a seizure in order to analyze its clinical signs, e.g. convulsions, neurological signs like fear or anger, pain, absence, because they are often related with onset zone. But the most important instrument to formulate a careful diagnosis is the brain electrical activity recording. There are four modalities to record electrical signals from brain:

- *Scalp electrodes (EEG)* are the least invasive method, but with

a lot of disadvantages. (a) Low spatial resolution on the scalp. (b) EEG determines neural activity that occurs below the upper layers of the brain (the cortex) poorly. (c) It requires precise placement of dozens of electrodes around the head and the use of various gels, saline solutions, and/or pastes to keep them in place. (d) Signal-to-noise ratio is poor [17].

Figure 1.2: An example of how electrodes should be put for a scalp EEG recording

- *Epidural electrodes* are used infrequently and generally only for lateralization and approximate localization of seizure onset. These electrodes are placed through tiny openings in the skull with the electrode contact resting on the dura to provide a high amplitude EEG signal without muscle or movement artifact. Because they do not penetrate the dura the risk of infection is minor. These electrodes can only record from the lateral convexity of the cerebral hemispheres and therefore are limited in their spatial resolution [18].

- *Subdural electrodes* are placed subdurally on the surface of the brain in the form of rectangular grids or linear strips with flat metal contact points mounted in flexible plastic. The grids require a craniotomy for placement and therefore are limited to unilateral application. The strip electrodes can be placed

through burr holes over the lateral convexity or under the frontal or temporal lobes. It is difficult to place them in the interhemispheric fissure to record from parasaggital regions because of technical risks associated with large cortical veins. The major advantage of subdural electrodes is that they do not penetrate cerebral tissue and can record from a relatively wide area of the cortical surface. They can also be used for extraoperative cortical stimulation to map out specific areas of cortical function. Unfortunately, subdural electrodes cannot record directly from the deep cerebral structures (i.e. amygdala, hippocampus and cingulum) which are characteristically involved in many medically refractory partial epilepsies. They also have a small but real risk of intracranial infection and hemorrhage estimated to be approximately 4% [19].

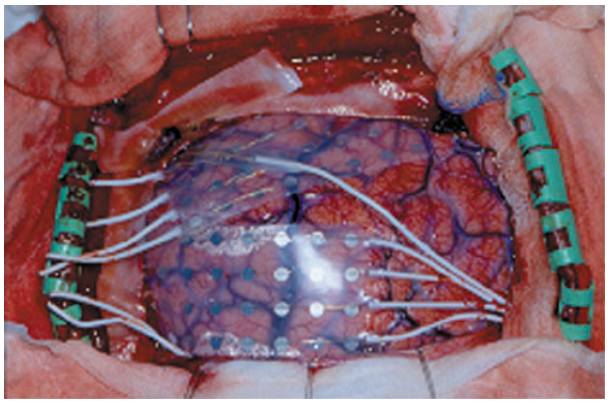

Figure 1.3: Subdural electrodes implanting.

- *Intracerebral depth electrodes* can be placed stereotactically into deep cerebral structures with the aid of CT, MR and angiography. Most centers employ flexible electrodes with multiple contact points that are placed through small holes in the skull and secured with some form of cranial fixation. Electrodes are usually targeted towards the amygdala, hippocampus, orbital-

frontal and cingulate regions and may be inserted via a lateral or vertex approach. Using a lateral approach, stereotactic cerebral angiography must be utilized to avoid major blood vessels during placement of the depth electrodes. Depth electrodes may be used in combination with scalp or subdural electrodes for more extensive coverage. Depth electrode investigation is generally indicated for patients with bitemporal, bifrontal of frontal temporal seizures and can localize a focal area of seizure onset not possible with scalp recordings. The major complications of depth electrodes include hemorrhage and infection with mortality and morbidity rates between 1 - 4%. It should be noted that the intracranial monitoring incurs greater risk than resective surgery itself and is also considerably more expensive than a noninvasive evaluation and therefore should be used only when necessary [20].

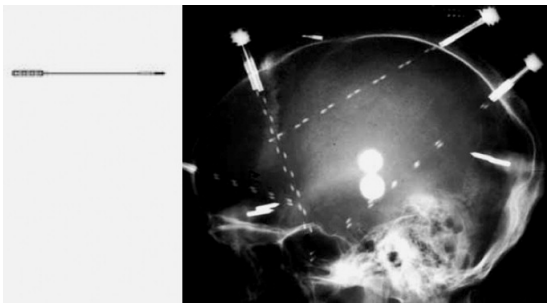

Figure 1.4: *Left*: *StereoElectroEncefalographic* electrode. *Right*: Post *StereoElectroEncefalographic* electrodes implanting radiography.

The recorded signal is visual inspected, especially the temporal windows containing the transition from the pre-ictal phase and the ictal activity, because this section of the signal usually presents clear epileptic electrical manifestation.

This work focuses on the information contained in StereoElectroEncefalographic (SEEG) signals (section 1.2) *, recorded with in-*

tracerebral depth electrodes, and especially on interictal signal.

1.2 StereoElectroEncephaloGraphic (SEEG) Signals

StereoElectroEncephaloGraphy (SEEG) is a diagnostic stereotactic procedure aimed at implanting recording multilead depth electrodes directly within brain structures, with a patient-tailored exploration strategy on the basis of noninvasive studies [21]. It is used in epileptic patients who don't respond to medical treatment, and who are potential candidates to receive brain surgery in order to minimize/dissolve seizures. Intracerebral electrodes are placed within the desired brain areas to record spontaneous seizures or to provoke them via low- and high-frequency stimulations, thus contributing to define with accuracy the epileptogenic zone, i.e. the site of the beginning and of primary organization of the epileptic discharge[22]. This technique was developed and introduced in the diagnostic iter of epileptic patients by Talairach and Bancaud at the S. Anne Hospital, Paris, France, in the second half of the 20th century [20]. Nowadays the basic concepts of this methodology are still valid, but modern technological tools facilitate the work-flow, as the integration of advanced multimodal imaging, obtained in frameless conditions, and robotic surgical implantation [23]. SEEG is a procedure aimed to localize epileptogenic zone with high accuracy and it is used only when EEG-VideoEeg and images (MRI, CT) are not enough for cortical ablation surgery planning. Unlike EEG, signals obtained have a good signal to noise ratio.

The electrodes implanted during SEEG procedures are semi-rigid multilead depth electrodes with 0.8 mm external diameter. Every contact is 2 mm long, with 1.5 mm inter-leads gap. These electrodes are available with 5, 8, 10, 12, 15, 18 contacts, without or with the

presence of groups of leads (3 groups with 5, 6 contacts each).

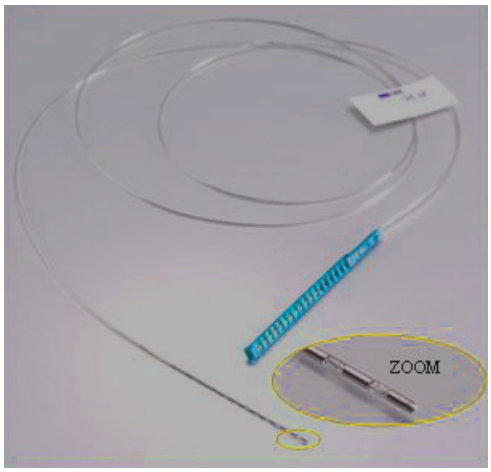

Figure 1.5: Multilead eletrode used for StereoElectroEncephaloGraphic procedure. On the right-bottom corner a zoom of the terminal leads

Each lead records electrical activity from a confined neuronal population in two different modalities:

1. Monopolar recording, where the voltage is measured respect to a "ground reference potential".

2. Bipolar recording, where the voltage of each leads is measures respect to another close lead. Usually bipolar signals are obteined with a difference between the difference of the voltage of recording of two consecutive leads.

1.3 The aim of the work

In this project, the epileptogenic zone identification is based on the analysis of *interictal Stereo Electroencephalographic signals*. The epileptogenic zone (EZ), following the theoretical principle of stereo-EEG (SEEG) methodology [24], is considered here as the site of the beginning and of the primary organization of the epileptic seizures.

Stereo Electroencephalography (SEEG) is a technique which consists in the insertion of electrodes in the brain cortex with surgery. Each of these electrodes is made up of a number, from 8 to 15, of different leads, which can record electric activity of a small neuronal population. This technique allows to have a less noisy signal than the EEG one and a very high spatial resolution. Implantation of the electrodes lasts even for some weeks, and they record a very huge amount of data. SEEG procedure is used in order to localize with a very high accuracy the seizure triggering zone, during the pre-surgical planning phase when an eplipetic subject is a good candidate for a cortical ablation surgery. Removing the brain area which triggers seizures is the only available treatment for drug-resistant partial epilpesies. Nowadays the analysis of the signals is performed manually by clinicians. The task takes a long time, and, for a correct epileptogenic zone detection, it's required at least one recording of the seizure. The aim of the work is to provide an automatic method to classify SEEG interictal signals in EZ (Epileptogenic Zone), namely recorded from a SEEG lead put within a epileptogenic neuronal population, and in NEZ (Non-epileptogenic Zone).

1.4 Outline of the thesis

The thesis is organized as follow:

- Chapter 2 summarizes the existing automatic algorithms aimed to the localization of the Epileptogenic Zone (EZ) and describes analytical methods for the evaluation and the analysis of networks and their connectivity properties.
- Chapter 3 describes the pipeline implemented for the automatic classification of the SEEG leads.

- Chapter 4 reports the performance of the implemented classifier using data of post-resected patient with seizure-free outcome.
- Chapter 5 concludes the thesis and presents possible developments for the presented work.

Chapter 2

State of the Art

2.1 Methods for automatic Epileptogenic Zone identification

To solve the problem of the epileptogenic zone (EZ) localization, during the last 50 years, a lot of trials were done. Anyway the problem is still alive, because none of the developed methods is able to replace the capacity and the experience of clinicians.

Most of this methods is based on the automatic analysis of bioimages (CT, MIR, PET, SPECT), in order to find some anatomical or functional abnormality. This kind of approach has some critical points. First of all, epilepsy is not always correlated to a visible lesion. Surely, in a subject affected by a certain type of cortical displasya, is often easy to find out the epileptogenic focus, because it very recognizable analyzing grey values in a MRI. But only a minimal number of epileptic subjects is affected by this kind of pathology. In all of the other cases the cortical malformation is more difficult to be localized and it may not totally fit with the epileptogenic focus.

To overcome the problems above, a trial with FDG-PET images, which measure the metabolic activity of brain regions, was done by Wesley et al. [25]. They have developed an automated computer-

aided diagnostic tool that has the potential to work both independent of and synergistically with expert analysis. Their tool operates on distributed metabolic changes across the whole brain measured by iPET. The algorithm is made by two part. The first one consists of the segmentation of PET images and of the computation of the average radioactivity in each Region of Interest (ROI), normalized by the whole brain radioactivity, as feature for the next step. The second part of the algorithms is based on a Multi-Layers Perceptron (MLP) aimed to each ROI classification. The MLP accuracy was 80%. Actually, due to the low resolution of the PET imaging technique, their CAD is able only to diagnose and lateralize temporal lobe epilepsy (TLE), making it inappropriate for a more accurate epileptogenic zone localization during a pre-resection planning.

Another study aimed to localize the epileptogenic zone using methabolic images was performed by Newey et al. [1]. They developed a very performant algorithm based on a SISCOM [26] coregistration between SPECT images and MRI. The specificity of the method is very high, around 90%, but the sensitivity is still too low (70%).

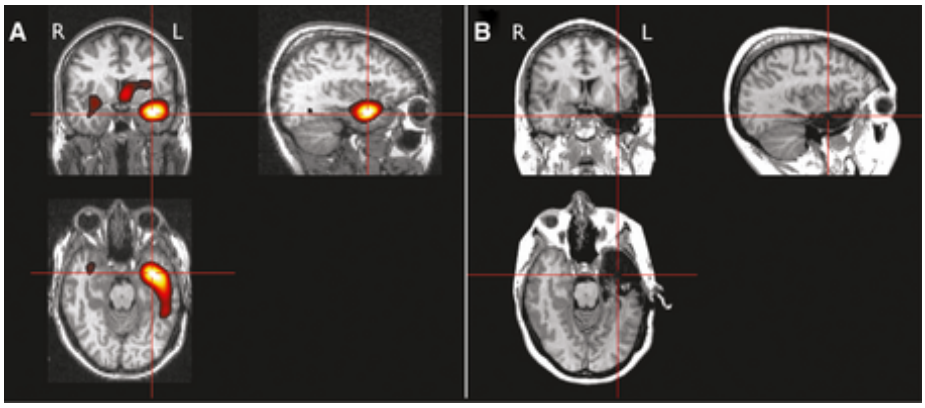

Figure 2.1: SISCOM analysis and MRI coregistration. *A* shows SISCOM analysis performed on preoperative MRI. *B* shows the coregistered postoperative MRI, which presents a resection consistent with SISCOM localization [1].

Although the algorithm cannot be used as a stand-alone automatic method, it could be a very useful tool in order to help neurologists in the epileptogenic zone localization task. But there is a big problem about the clinical application: Ictal SPECT is a cost-intensive and labor-intensive procedure reserved for the more challenging patients undergoing presurgical evaluation.

In a consistent number of cases the analysis of the images isn't enough, becuase there is not any evident cortical malformation and the epilepsy is caused only by an abnormal electrical activity, which is invisible to funcional images as well [27].

Then, in order to identify the epileptogenic zone, another approach consists in the analysis of the electrical activity of the brain. Over the past decades some trials were done to search a way to automatically identify a signal as epileptogenic with scant success. The reason of all this insuccess is that is impossibile to find a clear "epileptogenic pattern" in electrical signals due to the fact that there is an incredible number of different patology under the name of epilpesy. Only few information processing methods able to statistically characterize the spatio-temporal distribution of interictal transient events in large datasets have been reported up to now.

Nowadays the problem is still unsolved and the literature about SEEG/EEG processing for the epileptogenic zone identification is very brief.

One of the first profitable attempt was obtained by Wendling et al. ([28, 29]) with the estimation of the mutual involvement of different brain structures computing a non-linear non-parametric correlation h^2 index using the IEEG (Intracerebral EEG) signals. In particular the study was focused on the transition from pre-ictal activity to the seizure and on the ictal activity of patients with Temporal Lobel Epilepsy (TLE). It's reported that starting with the seizure onset, the computed correlation index of the involved

regions increses and its mean values is higher for the total duration of the ictal activity (see Figure 2.2).

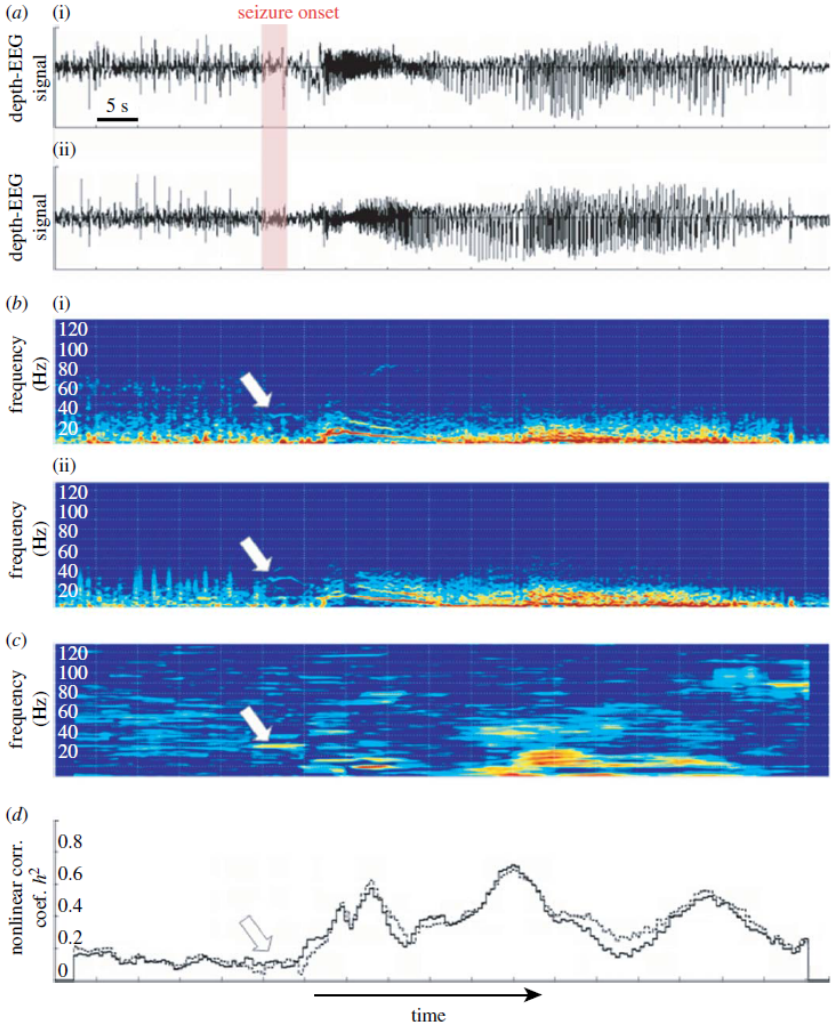

Figure 2.2: (a) Depth-EEG signals recorded from (i) amygdala (AMY) and (ii) hippocampus (HIP) in a human during transition to seizure activity in temporal lobe epilepsy. (b(i)(ii)) Spectrograms corresponding to depth-EEG signals obtained from short-term Fourier transform. (c) Estimated relationship between the two signals in the time–frequency plane, which reveals a synchronization process well localized in frequency at seizure onset. (d) Estimated relationship between the two signals using the $h^2(t)$ nonlinear regression analysis method. The increase of the $h^2(t)$ at the seizure onset denote the involvement of the Amygdala and the Hippocampus in the seizure (see [2]).

The study is a milestone in the EZ localization, because it showed that the epileptogenicity of different brain areas is strictily related to their mutual involvement with others. Anyway the method is not as much as reliable to an accurate EZ identification.

Another study focused on the mutual connection of different cortical areas, is reported by Bourien et al. ([30, 3]). They proposed a method able to analyze a particolar characteristic of the interictal signal. The method was based on three main task:

1. Automatic detection of monochannel itracerebral interictal spikes (mono-IIS).
2. Identification of multichannel intracerebral interictal spikes (multi-IIS).
3. Automatic extraction of Subsets of Co-Activated Strucures (SCAS) making use of data-mining and statistical test.

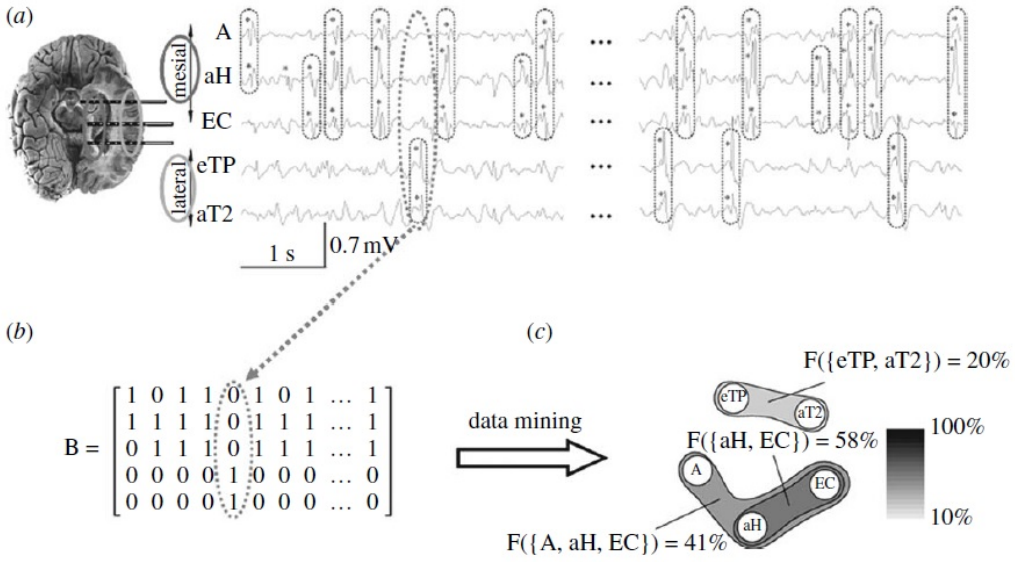

Figure 2.3: (a) Detection of mono-IIS and identification of multi-IIS in intracerebral EEG, (b) Boolean co-occurrence matrix and (c) extraction and representation of SCAS [2]. Method described in [3].

The interictal signal usually shows transient events (mono-ISS) which are one of the main feature that characterizes an epileptic IEEG. The detection of the IIS is a very critical aspect of this method, because, as shown in many studies ([31]), the ideal spike detector does not exist, as the specificity and the sensitivity remain difficult to control in a context where the frequency of spikes is modulated by the patient state and where the human experts have themselves difficulties, in some cases, to assess the presence of spikes. Bourien et al. used a technique based on wavelet decomposition that has proven particularly suited for enhancing transient signals well localized in time and frequency. After the detection of mono-ISS the method builds the matrix B which is a boolean matrix containing the co-occurance information extracted from the multichannel EEG data (identification of multi-IIS). Also this step has a critical aspect, beacuse the multi-IIS identification depends on sliding window, whose duration must be sufficientily short to avoid fusion of temporally unrelated monochannel events but it must be long enough to avoid the situation where temporally related events are not detected. Its duration was chosen experimentally. Then from the boolean matrix are extracted SCAS classifying all its subsets. Each SCAS come with a value which is the misure of the mutual involvement of the structures grouped in that SCAS. Higher values are correlated with an higher epileptogenicity. This task increases in complexity with the number of channel. Bourien's method isn't able to find the EZ with accuracy, but it can just provide a support to neurologists identifying the most probable epileptic triggering structures [2]).

In 2008 the Bartolomei's et al. [4] analyzed SEEG signals with a revolutionary method, described in the following. High-frequency oscillations are frequently observed during the transition from interictal to ictal activity, called *onset* window (Figure 2.4).

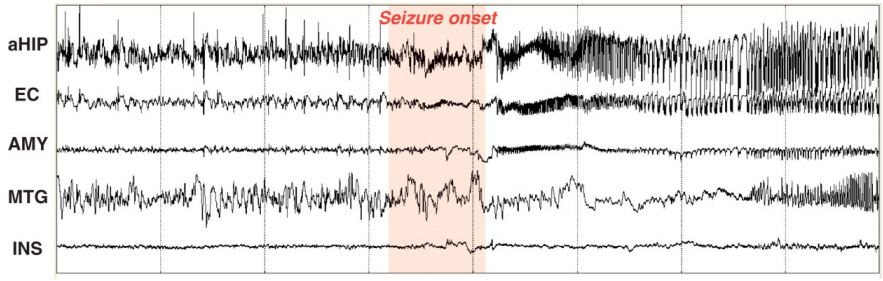

Figure 2.4: SEEG signals recorded in different brain cortical areas: anterior Hippocampus (aHIP), entorhinal cortex (EC), Amygdala (AMY), MiddleTtemporal Gyrus (MTG), Insula (INS). In the figure it's highlighted the seizure onset signal window [4].

They are often referred to as "rapid discharges" as they constitute a typical electrophysiological pattern characterized by a noticeable increase of signal frequency. Classically, the rapid discharge is a transient phenomenon, which lasts for a few seconds and which may or may not be associated with voltage reduction. In order to characterize both the propensity of a given brain structure to a rapid discharge and the delay of appearance of this discharge with respect to seizure onset, Bartolomei et al. [4] introduced a new index referred to as the 'Epileptogenicity Index' (EI). The purpose of this index is to provide quantified information about the behaviour of recorded brain structures from signals they generate during the seizure process (from onset to termination). This index summarizes two pieces of information into a single quantity:

1. Whether or not the recorded brain structure is involved in the generation of a rapid discharge.

2. When involved, whether or not this rapid discharge is delayed with respect to rapid discharges generated by other structures.

For the first time both frequency and time information were taken into account. Then it's possibile to assign to each signal an epileptogenicity index, which measure how much the zone from where the

signal has been recorded is epileptogenic. Anyway EI can be applied only for a limited number of epilpesy cases. In fact it works well only for very focal epilpesy type. Plus it's not always clear when EI is high enough to consider the related signal as epileptogenic. Among disadvantages, there is the problem that EI must be computed using the onset signal, not always available and with a decent signal to noise ratio. Plus, SEEG recordings are usually very extended in time and so, in order to compute EI, the algorithm must also be able to automatic detect the onset zone, which is a very critical task and an open-problem in the signal theory.

The first EZ localization study reporting also a sensitivity-specificity analysis was published in 2011 [5]. Dataset included 29 sublinical seizures and four seizure onset and it was made by SEEG recordings. It was analyzed with a functional connectivity index, Adapted Directed Transfer Function (ADTF), derived from the coefficients of a time-variant multivariate autoregressive model fitted to the data. ADTF was applied to each couple of SEEG channels. Different ADTF normalization was studied on simulations of ippocampal seizures and a Receiver Operating Characteristic (ROC) curve (figure 2.5) was computed. ADFT shows the source of a propagarion eletrical wave, making possibile the localization of the epileptogenic focus. The proposed method was validated on the dataset, made by 4 seizure onsets of 4 different patients and 29 subclinical seizures of the same patient. All the results obtained were concordant with post-surgical finding and it was concluded that the algorithm was able to correctly identify the hippocampus epilepsies without any history about seizure and patient.

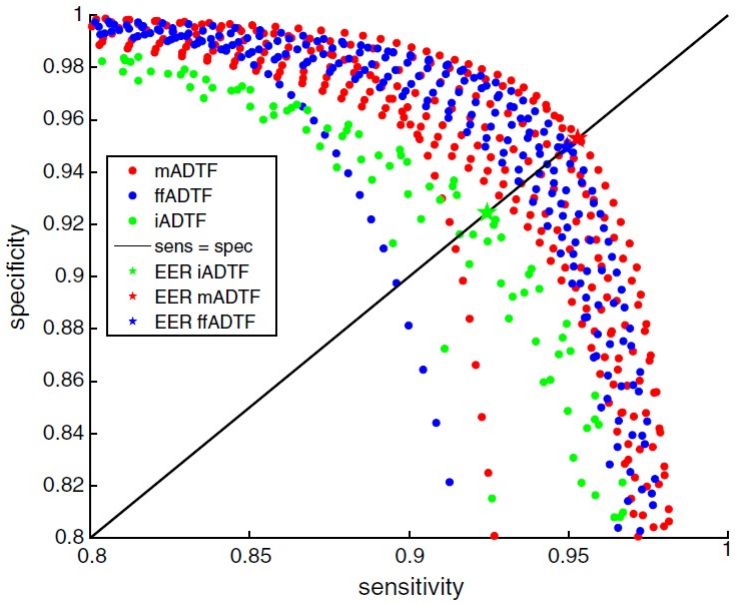

Figure 2.5: ROC curve of performances obtained with different normalization of ADTF in simulated seizure with added noise [5].

Chapter 3

Materials and Methods

SEEG leads were classified in EZ (epileptogenic) and NEZ (non-epilpetogenic) with a semi-unsupervised algorithm which searches similarities among the behaviour of each leads in a reconstructed brain network. Networks were reconstructed applying a non-linear non-parametric index to pairwised SEEG recordings.

The algorithm is made by two different sections:

1. Network analysis with the identification of the most significant subgraphs and the creation of a *"Role Fingerprint Matrix"*, a matrix aimed to describe the behavior of each lead in the network during time (sec. 3.2 and 3.3).

2. Clustering analysis on the "*Role Fingerprint Matrix*" data, in order to identify EZ and NEZ (sec. 3.4).

The first stage is based on the graph theory, especially on the finding of network paths which occurance is different from that in a respective random model. This kind of analysis is inspired by the new trend that the bioinformatic related to the study of genomic and proteomic is taking in these last years. The second stage is based on two methods of unsupervised classification.

Then, in section 3.5, is described an optimization problem aimed

to improve at best the classification performance.

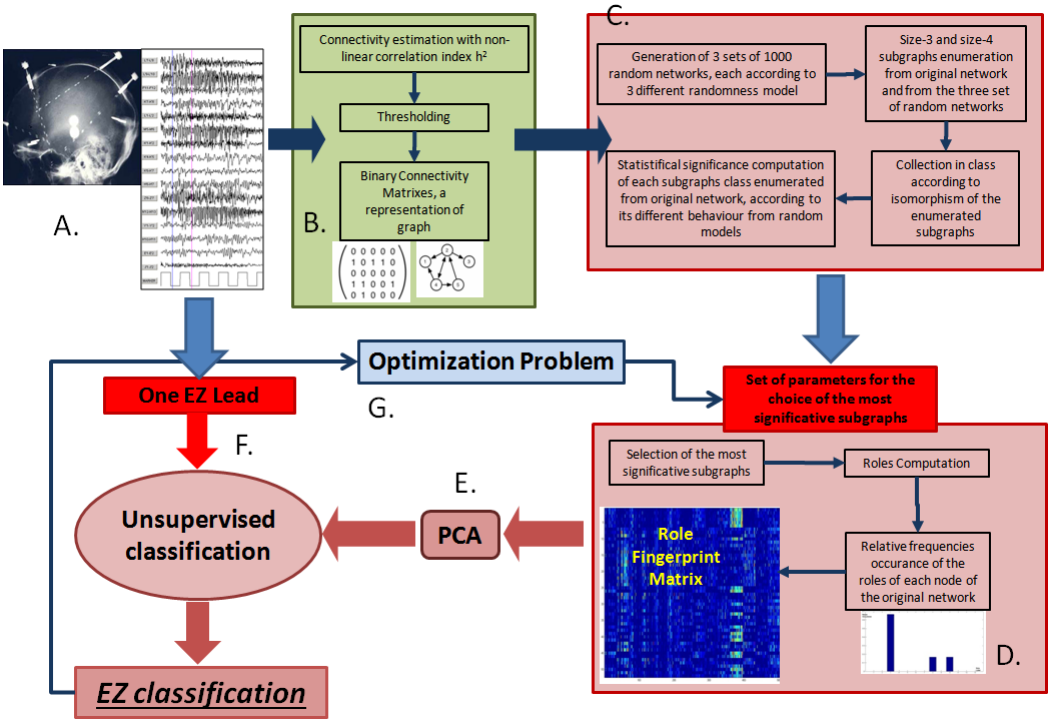

Figure 3.1: A recaping scheme of the implemented pipeline. A. SEEG signals are selected and labeled by a neurologist. B. Connectivity matrixes are computed in order to reconstruct the functional brain network. C. In the reconstructed network an algorithm searches subgraphs and assigns to them a measure of their statistical significance D. For each node (a row in the matrix in the picture) a set of ROLES is computed by the most significative subgraphs, on the base of the incoming and outcoming connections of the nodes. The selection of the most significative subgraph is made according to a set of parameters (U_3, Z_3, U_4, Z_4). The role information is stored in the Role Fingerprint Matrix. E. PCA on Role Fingerprint Matrix. F. The classification of the leads is based on unsupervised method, and the EZ leads are found providing to algorithm the information about just one EZ lead (using the labeling provided by neurologist). All the leads in the EZ cluster are considered positive, the others are considered negative (and so classified as NEZ). G. Optimization of the set of parameters U_3, Z_3, U_4, Z_4 used for the selection of of the subgraphs at point (D) They are optimized minimazing the False Negatives and then the False Positive of 4 FCD patients (using a priori information provided by clinician).

3.1 Connectivity Matrixes (A-B)

This stage of the algorithm corresponds to point A and B in figure 3.1.

There is the growing evidence that a wide range of neurologic disease are strictly related to the different connectivity behavior between brain areas [32, 33].

The dataset used in this work was made by connectivity matrixes provided by DDEP (Besta Hospital): SEEG recordings of each patient were divided into 36 non-overlapped 5 seconds-length epochs and each couple of channels was submitted to connectivity analysis by means of nonlinear regression method h^2 [34], a statistical measure that describes the dependency of a signal $y(t)$ on another signal $x(t)$ in a general way, independently of the type of relation between the two signals. This measure was called the correlation ratio $h^2(\tau)$. It is defined as follow:

$$h^2(\tau) = 1 - \frac{VAR\left[y(t+\tau)/x(t)\right]}{VAR\left[y(t+\tau)\right]} \tag{3.1}$$

where

$$VAR\left[y(t+\tau)/x(t)\right] \doteq \underset{h}{argmin} E\left[y(t+\tau) - h(x(t))\right]^2 \tag{3.2}$$

The h^2 index is asymmetric ($h^2\left(x \to y\right) \neq h^2\left(y \to x\right)$), and this interesting property which allows an investigation of whether h^2 is symmetric or not can give insight into the nature of the relationship between $x(t)$ and $y(t)$.

A Connectivity matrix (also reffered to as Adjacency matrix) was then built for each epoch, with the value of the element (i, j) representing the association or flow of information from channel $x_j(t)$ to $x_i(t)$, where each channel was a recording lead of a SEEG electrode (figure 3.2). Each element of diagonal of each matrix was equal to

zero, because the auto-connections (the dependency of a signal with itself) was ignored.

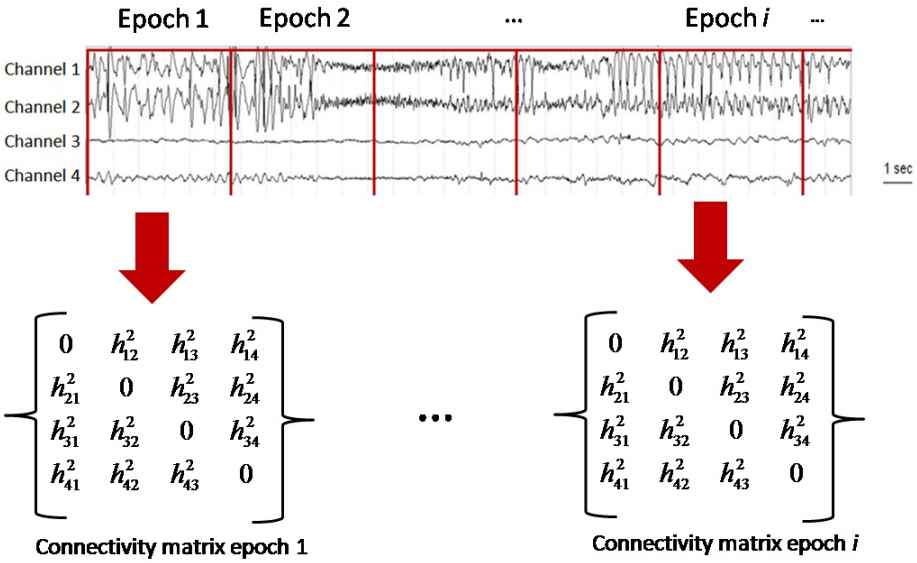

Figure 3.2: An example of how the connectivity matrixes were computed. For each epoch a different matrix was computed. Each element of the matrix is an h^2 signal between two channels of the SEEG recording. In this example only four channels were considered. Usually there are at least 30 channels.

Each value of the matrix is a h^2 index which measure the strength of the connection between two leads. For instance, considering the element in row 2 and column 1, h^2_{21} index, if its values is equal to 0.06, it means that the information flows from lead number 1 to lead number 2 with a strength equal to 0.06. Viceversa h^2_{12} index show the power of the connection from lead 2 to 1.

An example of a connectivity matrix could be seen in figure 3.3, where 84 leads are considered. It is the representation of the information flow of one epoch of SEEG signal of a Patient affected by Cortical Focal dysplasia of type II.

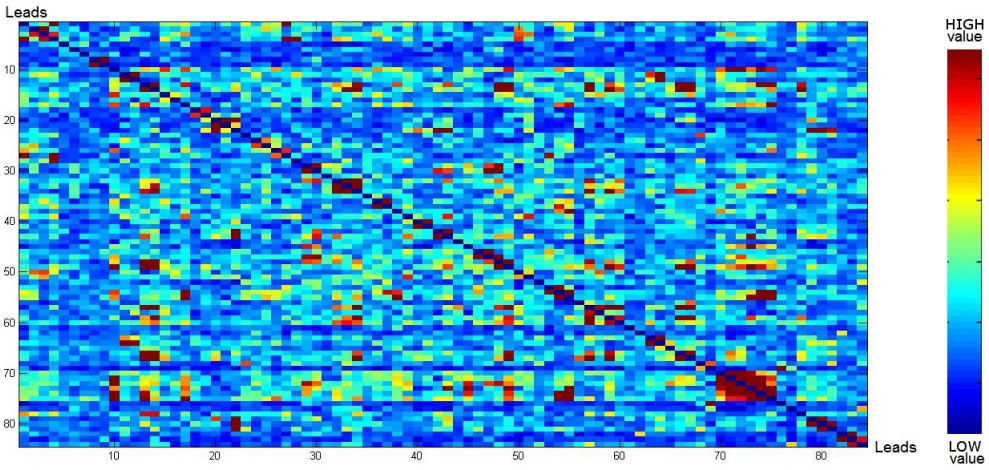

Figure 3.3: An example of the connectivity matrixes provided by DDEP. Each element is h^2index representing the connection power between two leads. Different colors are different h^2 values.

A connectivity matrix is a representation of the mutual dependencies of the neural processes recorded by the SEEG. Each connectivity matrix is the functional connectivity picture of the brain areas under study. For each patient 36 connectivity matrixes were computed, one for each epoch.

Then a threshold of h^2 was computed in order to build binary connectivity matrix.

The threshold $h^2_{threshold}$ is the minimum h^2 among the maximum of each lead. In figure 3.4 the complete threshold choice workflow is reported.

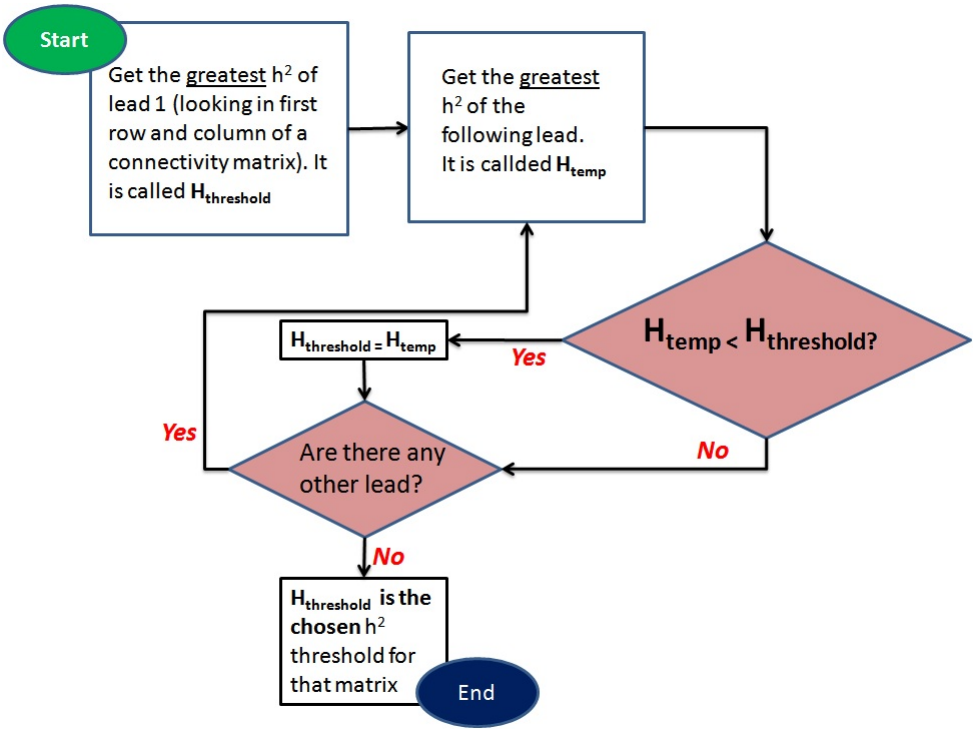

Figure 3.4: The workflow of how the threshold h^2 was chosen for each epoch.

Then for each matrix each $h^2 \geq h^2_{threshold}$ was replaced with a one, the $h^2 < h^2_{threshold}$ with a zero.

After the thresholding, each connectivity matrix became a *binary connectivity matrix*. A binary connectivity matrix is the representation of a graph.

Even if usually *graph* and *network* have a meaning slightly different, in this work the two words will be both used reffering to the same concept.

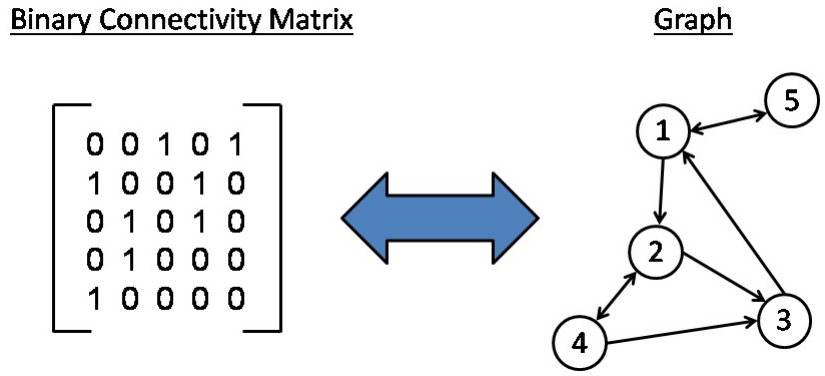

Figure 3.5: Equivalence between a binary connectivity matrix and a graph. In the figure it's considered a directed case, becuase fit with data used in this work

In figure 3.5 is shown the equivalence between a binary connectivity matrix and a directed graph. *Columns* represent the outward connections, *rows* the inward connections for each node of the related graph. Just to make an example, always looking at the figure 3.5, column 1 shows that the node 1 in the graph has two outward connections, one toward the node number 2 and one toward the number 5.

In the following, binary connectivity matrix will be simply called connectivity matrix. Symmetric connectivity matrixes are translated in *undirected graphs*, while asymmetric matrixes represent *directed graphs* (figure 3.6).

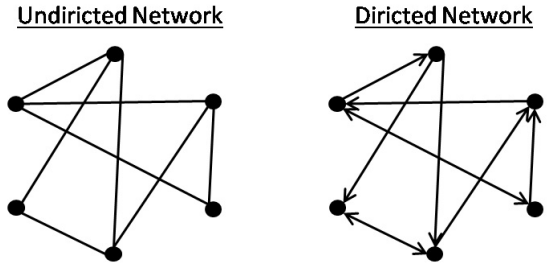

Figure 3.6: In undirected network the information flow isn't expressed. Usually the use of an undirected links is deprecated except when all the connections are bidirectional

Since h^2 index has the asymmetry property, in this work the methods proposed will handle directed graphs.

There were 36 (one for each epoch) binary connectivity matrixes (graphs) for each patient (figure 3.7). Each matrix is the representation of functional connectivity estimated from SEEG signals in each epoch.

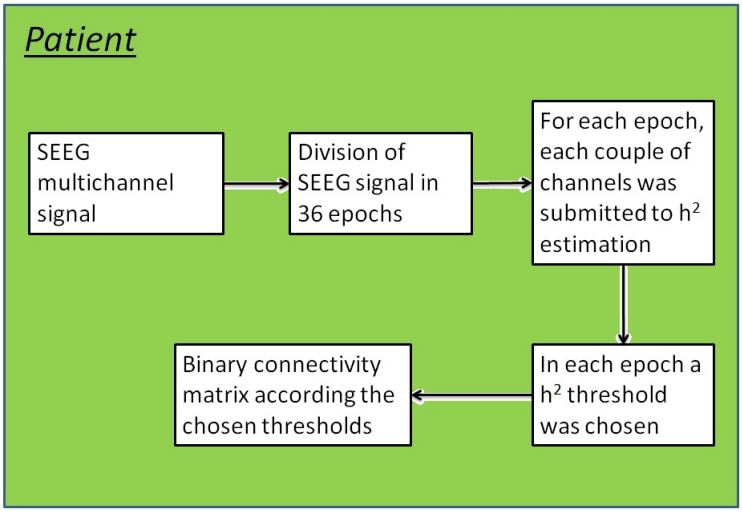

Figure 3.7: A summary of the workflow from the SEEG signals to the connectivity matrixes.

3.2 Network Analysis (C)

This section of the algorithm corresponds to point C in figure 3.1.

A large network can be subdivided in smaller structures made by k nodes, called *size-k subgraph*s, which represent subpaths in the networks circuits (figure 3.8).

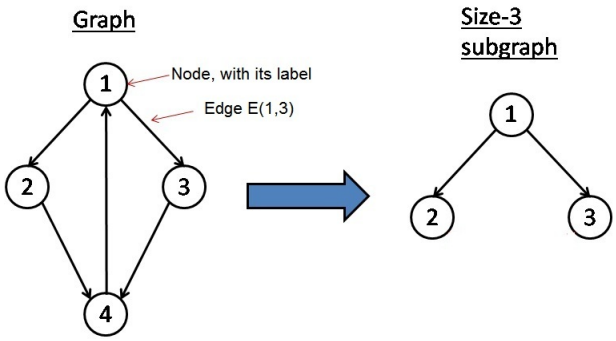

Figure 3.8: A Graph and a size-3 subgraph extracted from the given graph.

There are evidences that local subpaths in a network play a key role in the definition of the network properties [35, 36].

The first stage of this thesis was to perform a complete *network analysis* of the graphs described by the connectivity matrixes (section 3.1), aimed to find the most significative subgraphs, which should represents the connections not due to chance (noise).

The network derived from the connectivity matrix in the following will be called *original network*. From each connectivity matrix (original networks) three sets of 1000 random networks were genereted. The number of nodes of each random network is equal to that of the original network. Each set was builded according a different randomness model:

- *Local randomnes*s. In this model, unidirectional edges are only exchanged with unidirectional ones. The same applies for bidirectional edges. Therefore, the number of incident bidirectional edges remains locally constant, that is, it constant for each vertex.

- *Global randomness*. Model where the number of bidirectional edges is kept constant in the overall network. However, a specific vertex may lose or gain incident bidirectional edges.

- *No regard.* This states that bidirectional edges can be created and destroyed during randomization. This option usually increases the number of bidirectional edges compared to the original network.

In all cases, the random network is generated from the original network by a series of three edge switching operations (Figure 3.9). So the overall number of the inward and outward connections in the random networks is always the same of those in the corresponding original network.

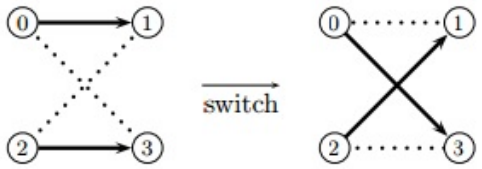

Figure 3.9: The random model used to estimate the the statistical significance of each graph are built switching the links different times.

From the original network and from each random network, all size-3 and size-4 subgraphs were enumerated using the ESU algorithm [37], a very efficient method able to accomplish the enumeration task of large networks in a short time.

Then, size-3 and size-4 subgraphs of each network (both the original and those of the three sets) were collected into labeled subgraph classes S_k, according to the isomorphism (figure 3.10) criterium. To accomplish this task was used the Nauty algorithm [38, 39, 40] (see appendix A).

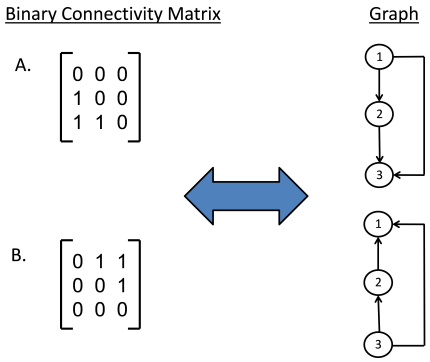

Figure 3.10: Feed Forward Loop is a very recurrent subgraph in the biological systems. In the figure are shown two of its *isomorphic* states. On the left the connectivity matrixes and on the right the corresponding graphs.

At this point each network (both the original and those of the three sets) was accompanied by its own collection of size-3 subgraphs grouped into subgraph classes (S_3) and by its own collection of size-4 subgraphs grouped into subgraph classes (S_4).

The significance of each class is based on statistical measures, computed as follow. Let's consider the *original* network, which is that derived from connectivity matrixes described in section 3.1, and the large set of *random networks.*

Classes S_k enumerated from the original network and in the set of random networks are the same, because it's possible to find a confined set of different classes, depending on the size (k) of the subgraphs considered. Then for each S_k were computed the occurance frequency $f_{original}$ in the original network and the mean occurance frequency $\bar{f}_{random}$ of the random model over the set of random networks.

$$f_{original}(S_k) = \frac{length\{S_k\}}{N_{subgraphs}} \tag{3.3}$$

where S_k is the set of the enumereted subgraphs grouped into a certain subgraph class and $N_{subgraphs}$ is the total number of sub-

graphs enumerated in the whole original network.

$$\bar{f}_{random}(S_k) = \frac{1}{N_{random}} \sum_{i=1}^{N_{random}} \frac{length\{S_k^i\}}{N_{subgraphs}^i} \tag{3.4}$$

where:

- N_{random} is the number of random network generated.
- S_k^i is the set of the subgraph with a certain label found in the i-th random network.
- $N_{subgraphs}^i$ is the total number of subgraphs enumerated in the i-th random network.

In this work $N_{random} = 1000$.

Using these frequencies a z-Score for each class is computed, which is a normalized measure of the deviation of a S_k from a random model:

$$zScore(S_k) = \frac{f_{original}(S_k) - \bar{f}_{random}(S_k)}{std(f_{random}(S_k))} \tag{3.5}$$

The final output is a list of all the size-k subgraph (with k=3 and k=4) classes S_k found in the original network analyzed, accompanied by their relative $f_{original}$, $\bar{f}_{random}$, $zScore$. This method was applied to connectivity matrixes stored in the dataset, i.e. for each epoch in which SEEG signals were divided, and for each patient. Obviously the obtained values of $f_{original}$, $\bar{f}_{random}$, $zScore$ were different for each epoch. Due to the computational time, which scale with the increasing of the size of subgraphs and according to the number of nodes in the original network, the algorithm was applied only to search size-3 and size-4 subgraphs.

Each patient, which is represented by a collection of 36 binary connectivity matrixes, underwent to a total network analysis (figure 3.11): from each one of the 36 connectivity matrixes (original net-

works) three, one for each randomness model, sets of 1000 random networks were generated. Then from each of the 36 original networks and from its related sets of random networks, are enumerated size-3 and size-4 subgraphs. Then they were collected into classes S_k according to the isomorphism criterium. For each class of each original matrix two statistical parameters were computed ($f_{original}$ and $zScore$).

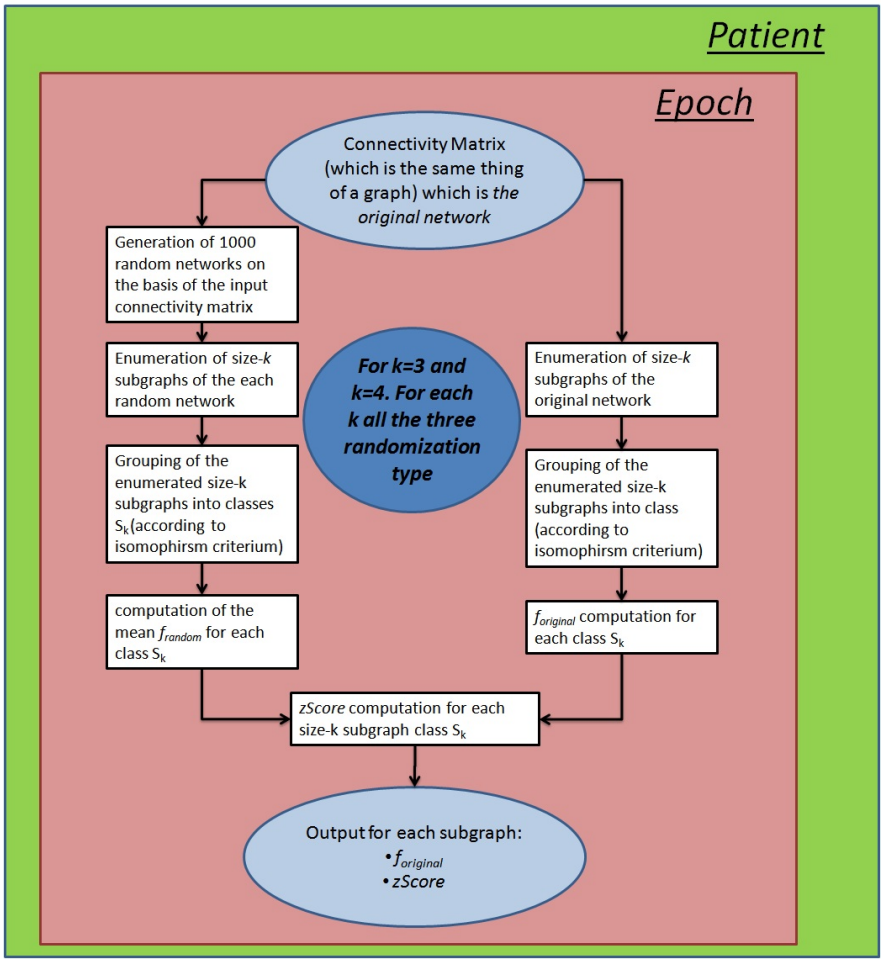

Figure 3.11: Network analysis described in detail. It is performed for each of the 36 epoch (of each patient).

At the end of this stage each enumerated subgraph from each of the 36 original networks were recorded into a Database. There is a file for each epoch and for each patient. Each record in these files contains the following information:

- Leads involved in the size-k subgraph. They are labeled according to their position in the conncectivity matrixes.
- An ID of the related $S_k$subgraph class. It's a unique number assigned to each subclass class found in order to uniquely identify it.
- The class related $f_{original}$ and $zScore$ values.

Node A	Node B	Node C	$S_k\, ID$	$f_{original}$	$zScore$
4	10	34	12	0.06	0.4

Table 3.1: An example of how each subgraph found in the original network is recorded. In this example a size-3 subgraph is considered. First three column (Four if the considered subgraph has three nodes) are the label of the Lead involved in that subgraph. Then the last three columns are the ID of the subgraph class in which the leads are involved, the occurence frequency of the subgraph and its z-score.

In table 3.1 there is an example table. It describes the representation of an enumerated subgraph from the original network. For each epoch there are a variable number of enumerated subgraphs (records), whose order of magnitude is the following: for size-3 subgraphs there are 10^5records and for size-4 subgraphs 10^6.

For the implementation of the above algorithm used FANMOD's libraries [41] , compiled and runned in a GNU/Linux environment. The algorithm was wrapped in a parallelizing C++ coded structure (non-CUDA) in order to reduce the computation time. Unfortunately the method requires a large amount of memory, due to the dimensions of the network analyzed. So only two thread could be executed at the same time without the overhanging within the swap memory (with a great drop in performance).

3.3 Roles Fingerprint Matrix computation (D)

The following procedure corresponds to point D in figure 3.1.

Each subgraph recorded was considered significative if its subgraph class S_k has the following characteristics:

- $f_{original}(S_k) \leq U$
- $|zScore(S_k)| \geq Z$

Where *U is a frequency threshold* and *Z is a z-Score threshold.*

U and Z are parameters chosen solving an optimization problem (see 3.5). All the subgraphs, whose subgraph class was not considered significative, were discharged.

The purpose of the method proposed in this thesis is the calssification of the SEEG leads in EZ (epileptogenic) and NEZ (non-epileptogenic). Epileptogenic EZ are a confined subset of the total lead number. The hypothesis formulated is that each size-k subgraph represents a little piece of information concerning the system under study. In the case of the network built up with SEEG recording, the information carried by each subgraph concerns how each neuronal populations talks with the others. According to this hypothesis the most frequent subgraphs carry the information common to a large subset of the network nodes (leads). Since the epileptogenic network involves only a very small subset of nodes, the information about EZ must be searched in the rarest subgraphs, selecting only the classes with their occurance frequency $f_{original}$ under a certain threshold. At the same time, selected subgraphs must have a $zScore$ higher enough to consider their occurance different from those in a random network. $S_k$with a $zScore$ too close to zero can be considered as random noise [36].

From each significant S_k, selected according to the constraints described above, another group of features were extracted, called in this work ROLES.

Given a binary connectivity matrix A^k of a size-k subgraph class, its element are marked with $a^k_{ij}$where i and j must be included from 1 to k. A ROLE is a set of four numbers:

$$ROLE = \{ID, k, In, Out\} \tag{3.6}$$

where

- *ID* is a unique identification number given to each size-k subgraph class. Its only purpose is to identify each class of S_k uniquely.
- k is the subgraph dimension.
- *In* and *Out* are the In Degree and the Out Degree of the role, i.e. the number of inward and outward connection of each single node in the subgraph under analysis. They were respectively computed as in the equation 3.7 and 3.8.

$$Out(i) = \sum_{j=1}^{k} a_{ij} \tag{3.7}$$

$$In(j) = \sum_{i=1}^{k} a_{ij} \tag{3.8}$$

Roles have two properties, which limit their number in given size-k subgraphs.

Property 1. For a given size-k subgraph class, exists at least one role.

There is only one role, for instance, in symmetric cyclical graphs (figure 3.12).

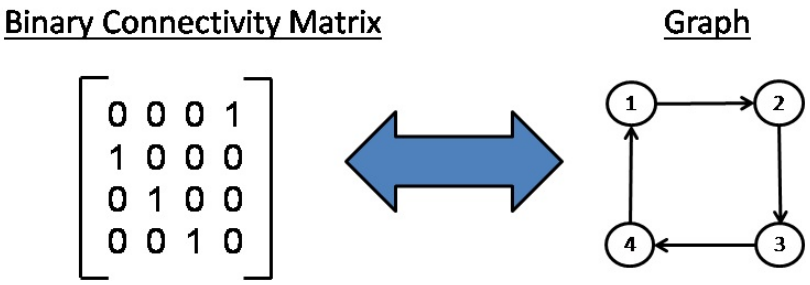

Figure 3.12: An example of a graph where all its nodes have the same roles. In this example all nodes have one inward connection and one outward connection. This is a symmetric cyclical graph.

Property 2. For a given size-k subgraph class there are maximum k different roles.

It happen when all nodes have a different role (figure 3.13

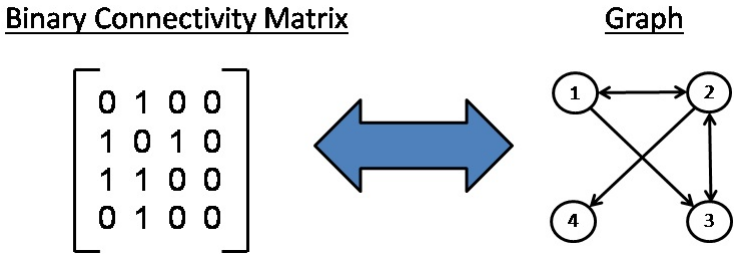

Figure 3.13: A graph where each node has a differrent roles

Thanks to the previously described properties, it is possible to create a list of all the roles identified in each epoch of each patient, in order to have a common dictionary for any new elaboration. The dictionary allows the coupling of a single identification number IR to each role, giving an easier instrument to manage roles. The dictionary is defined as a biunique function D:

$$IR = D(ID, k, In, Out) \tag{3.9}$$

Such function has been implemented in a SQL data structure and each of its instance is a SQL query.

In the following, in order to clarify the concept of role and how the Dictionary function works (equation 3.9), will be provided an example.

Considering the size-4 subgraph A^4(figure 3.14). Subgraph $A^4$is enumerated from a larger network. It's a assigned to a class S_k with $ID = 137$. Then $f_{original}$ and $zScore$ of $A^4$are computed.

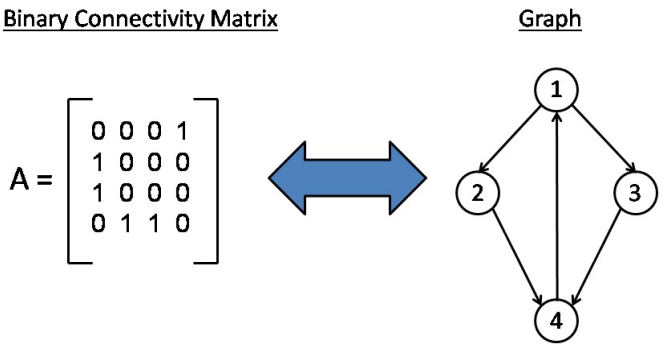

Figure 3.14: A size-4 subgraph and its relative connectivity matrix A^4

Assuming that its $f_{original} \leq U$ and $|zScore| \geq Z$ and so it was considered significant. Each node is represented by a row and column with "the same number". For example, node 1 is represented by the first row and first column, node 2 by the the second row and second columns, and so on. Equation 3.7 and 3.8 are applied to the matrix and to each node is assigned a set of number (definition 3.6). The table 3.2 is related to the example in figure 3.14:

Node Label (see figure 3.14)	ID	K	In	Out
Node 1	137	4	1	2
Node 2	137	4	1	1
Node 3	137	4	1	1
Node 4	137	4	2	1

Table 3.2: Example of definition of roles with 4 definition numbers

These data are used as input for Dictionari Function D (Equation 3.9) obtaining an IR for each node:

Dictionary Function	Function Output (IR)
$D(137, 4, 1, 2)$	450
$D(137, 4, 1, 1)$	451
$D(137, 4, 1, 1)$	451
$D(137, 4, 2, 1)$	452

Table 3.3: Working example of the dictionary function

The function D sends a query request to the SQL database for each combination of four parameters. If the combination already exists, the IR is simply returned and assigned to the node. If the combination doesn't exist, the Dictionary Function adds a new record to the database with an IR increased by one compared to the maximum already existing.

For each subgraphs enumerated during the first subtask from the real network a roles computation was performed.

Let's consider only a patient and only one epoch (one connectivity matrix) related to it. The algorithm described above was runned, obtaining for each network node (the representation of the SEEG leads) a list of roles, each role identified by a unique number (IR). Each node can assume more than one role at a time, because it can be involved in a large number of different subgraphs at the same time. Then, for each node, a frequency histogram is computed (figure 3.15), counting how many time each role occurs.

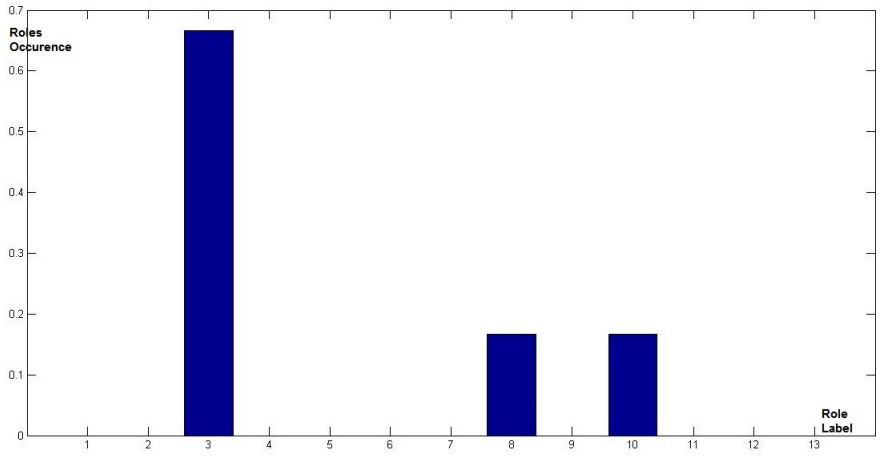

Figure 3.15: Size-3 roles histogram of the lead number 9 of the patient 5 in epoch 3. On the x-axis role IR (in this case from 1 to 13) and on the y-axis the occurance frequency normalized between zero and one. It is the representation of the behavoiur of a SEEG lead in the reconstructed network during one epoch. Each lead will have 36 histogram like the one in the picture.

In figure 3.15 there is the occurence histogram of the roles assumed by a single node, considering only size-3 subgraphs.

Then the histogram was normalized between zero and one. A histogram was computed for each epoch. At the end of this stage, each node had 36 (the number of epochs) different histograms, which describe a sort of *"fingerprint"* of the roles that a node can assume over time. The output of this stage is a matrix for each patient, whose rows are the nodes of the graph estimated by the pairwised SEEG channels (leads), and whose columns are the values of the 36 histograms for each lead, that are put side by side. Such matrix has been called *Roles Fingerprint Matrix* (figure 3.16). The number of columns of this matrix depends on:

- The number of subgraphs classes considered significative.
- Size of the subgraphs considered. Can be considered size-3 subgraphs, or size-4 subgraph or both togheter.

- The randomness model considered. They can be used separately, pairwised or also all togheter.

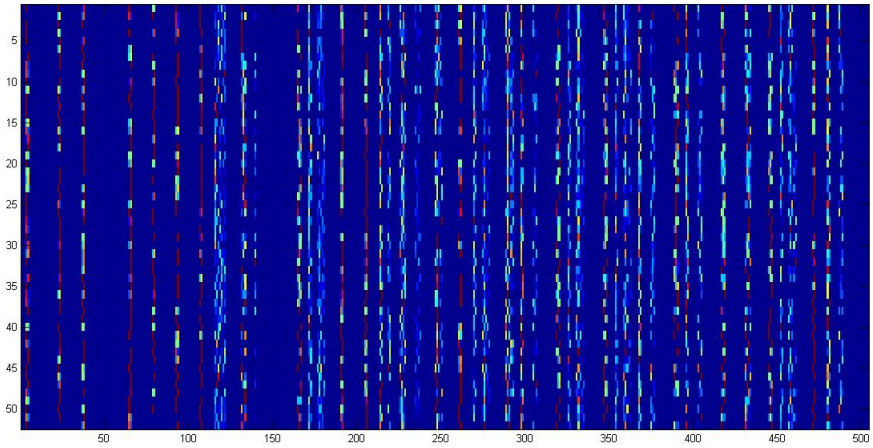

Figure 3.16: *Roles Fingerprint Matrix.* Each row represents a lead and on the column there are the role occurance, derived from histogram, over the epochs. Red color means high occurence, blue means low occurence.

For each patient 18 different Roles Fingerprint Matrixes were computed. Each of them was obtained with a different combination of the dimensions of the subgraphs and/or different combination of random model (see list in chapter 4).

3.4 Unsupervised Classification (E-F)

This step of the algorithm corresponds to point E and F in figure 3.1.

The output of the algorithm described in the previous section is a matrix (Roles Fingerprint Matrix) where each line contains all the features (roles occurrance over time) extracted with the network analysis. Each line is a vector, which can be the input of a classification method. Each vector represents a SEEG lead, which have to be classifed in EZ and NEZ (figure 3.17).

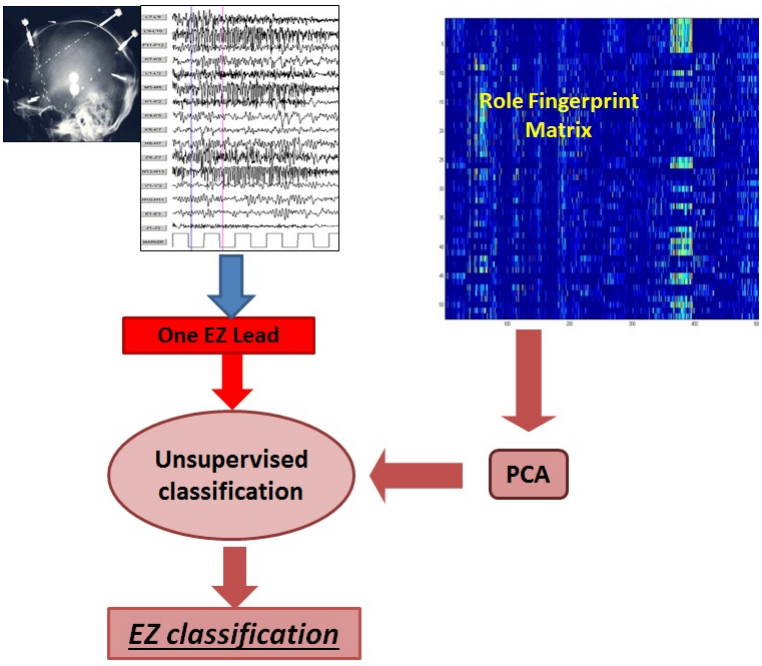

Figure 3.17: Workflow of the clustering analysis

The problem is that the vector has very large dimensions (till to 30000 dimensions), due to the great number of roles that can be found, especially in size-4 subgraphs.

The majority of the classification/space partitioning algorithm are not so robust when inputs have too many dimensions, and there is the risk that the computation time increases esponentially. In order to reduce these problems the dataset obtained at the end of section 3.2 (the Roles Fingerprint Matrix) was first elaborated with Principal Component Analysis (PCA) (E in figure 3.1) in order to reduce its dimensions. Principal component analysis (PCA) is a mathematical procedure that uses an orthogonal transformation to convert a set of observations of possibly correlated variables into a set of values of linearly uncorrelated variables called principal components. The number of principal components is less than or equal to the number of original variables. This transformation is defined

in such a way that the first principal component has the largest possible variance (that is, accounts for as much of the variability in the data as possible), and each succeeding component in turn has the highest variance possible under the constraint that it be orthogonal to (i.e., uncorrelated with) the preceding components. The explained variance took into consideration was the 99%. Even if the cutoff of the variance was so high, dimension of dataset always decreased from about 30000 to about one hundred dimensions.

Then two kinds of clustering were used: *K-Means Clustering* and *Affinity Clustering* (F in figure 3.1).

The choice of an unsupervised partition method is a bit unusual in a binary classification like the one in this thesis. Actually, even if the purpose is the partition of the leads in two classes, EZ and NEZ, it's only an approximation. A deeper reflection about the choice of the classification method will be done in Chapter 5.

To accomplish the classification, after the clustering, will be provided to the algorithm just one EZ lead. The cluster containing that EZ lead, will be considered the EZ cluster CL_{EZ}, and all the leads owning to that partition will be considered as EZ. Then, in order to estimate the performance, will be measured the False Negative (FN) 3.10, the False Positive (FP) 3.11 and the True Positive (TP):

$$FN = length\left\{LEAD_{EZ} \notin CL_{EZ}\right\} \tag{3.10}$$

$$FP = length\left\{LEAD_{NEZ} \in CL_{EZ}\right\} \tag{3.11}$$

$$TP = length\{LEAD_{EZ} \in CL_{EZ}\} \tag{3.12}$$

where $LEAD_{EZ}$ is the subset of the overall lead set labeled by the neurologist as Epileptogenic and $LEAD_{NEZ}$ is the subset labeled as Non-Epileprogenic.

False Negative and False Positive will be also be expressed in percentage (False Negative Rate FNR 3.13 and False Positive Rate FPR 3.14):

$$FNR = \frac{FN}{length\{LEAD_{EZ}\}} \tag{3.13}$$

$$FPR = \frac{FP}{length\{LEAD_{NEZ}\}} \tag{3.14}$$

In order to evaluate performance with more compact measure was used the Accuracy:

$$Accuracy = 1 - \frac{FN + FP}{N_{leads}} \tag{3.15}$$

where N_{leads}[1]is the total number of the leads classified in that patient.

Finally another index, F-Score, was computed:

$$F = 2 \cdot \frac{precision \cdot recall}{precision + recall} \tag{3.16}$$

where:

$$precision = \frac{TP}{TP + FP} \tag{3.17}$$

$$recall = \frac{TP}{TP + FN} \tag{3.18}$$

F-Score is aimed to measure how much a linear classifier (EZ/NEZ) works well for both the classes. It ranges from zero to one and higher it is, better are performances on both classes.

The classifications obtained with the two clustering method were compared with the chi-squared test. The null hypothesis H_0 was: <<Have the two method the same classification performance?>>

[1]Formal definition: $N_{leads} = length\{LEAD_{EZ} \cup LEAD_{NEZ}\}$

The confidency level desired was $\alpha = 0.001$. The tabled value according to α $is \chi^2_{crit} = 10.83$.

3.4.1 K-Means clustering

In statistics and machine learning, K-Means clustering is a method of cluster analysis which aims to partition n observations (in this work each vector of *"role features"* representing a lead) into k non-empty, non-overlapping and non-subordinated clusters, in which each observation belongs to the cluster with the nearest mean. In its most common form, the algorithm is an iterative greedy algorithm which converges to a local optimum after a certain number of iterations.

The algorithm works by first selecting k locations at random to be the initial centroids for the clusters. Each observation is then assigned to the cluster which has the nearest centroid, and the centroids are recalculated using the mean value of assigned values. The algorithm then repeats this process until the cluster centroids do not change anymore, or until the change less than a given threshold.

To avoid local minima the algorithm was repeated 20 times and the clustering with the minor distance within cluster was chosen.

The pairwise distance used was a correlation distance, defined as following:

$$D_c(x, y) = 1 - \frac{(x - \bar{x})(y - \bar{y})^T}{\sqrt{(x - \bar{x})(x - \bar{x})^T}\sqrt{(y - \bar{y})(y - \bar{y})^T}} \tag{3.19}$$

Where x and y are two vector representin two leads.

The correlation distance doesn't measure the absolute distance between two vectors, but it focuses on how much the components trend of the two vectors is similar. Such choice was taken because the attention was putted on the change during time of the behaviour of the nodes, ant not on each single component of the roles vector.

The reason is that epileptogenic regions usually show in time little changes in their relation with other brain zones [33, 2].

K-Means clustering have a main issue, which consists in the difficult choice of the number of clusters that the algorithm have to generate.

3.4.2 Affinity Propagation

Affinity propagation is an algorithm that identifies exemplars among data points and forms clusters of data points around these exemplars. It operates by simultaneously considering all data point as potential exemplars and exchanging messages between data points until a good set of exemplars and clusters emerges [42]. An *exemplar*: is a data point, in this case a lead, that is nicely representative of itself and some other data points. It means that the lead fingerprint identified as *exemplar*, become a sort of label for a set of leads.

Affinity propagation is based on the concept of *similarity*, which is the opposite of the concept of *distance* (used for example in the k-means clustering). The *similarity* of data point x to data point y, called $s(x, y)$, is the suitability of point y to serve as the exemplar for data point x. Similarity can be expressed with different king of metric. Since in this work data are real-valued, the similarity was measured with negative *Euclidean Distance*:

$$s(x, y) = -[x - y] \cdot [x - y]^T \tag{3.20}$$

where x and y are two input vectors.

To each input data point has assigned a *preference* value. The *preference* of a point i, called $p(i)$, is the a priori suitability of point i to serve as an *exemplar*. Preferences can be set to a global (shared) value, or customized for particular data points. High values of the preferences will cause affinity propagation to find many exemplars (clusters), while low values will lead to a small number of exemplars

(clusters). A good initial choice for the preference is the minimum similarity or the median similarity. In this work, the preference was set globally equal to the minimum similarity, because an higer value would have led to a too large number of cluster. In fact one of the main advantage of this method is the automatic choice of the number of cluster.

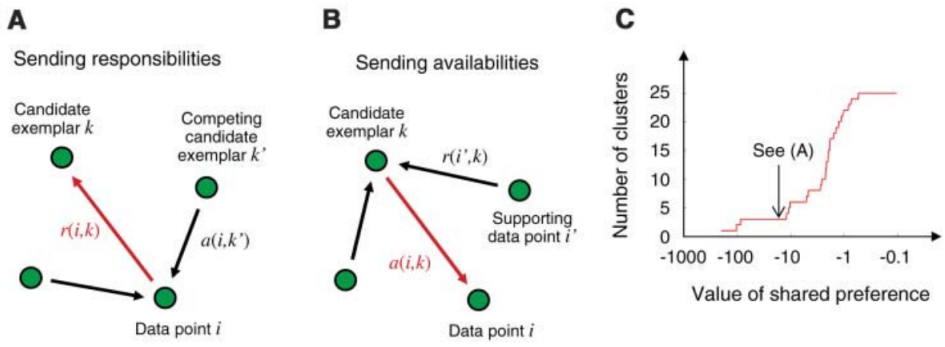

Figure 3.18: A. How *responsability* $r(i,k)$ communicate with data points. B. *Availability* $a(i,k)$ working. C. Trend of the number of cluster in function of *preference* $p(i)$.

Affinity Propagation works exchanging two type of messages between data points:

- *Availability*: Message sent from candidate exemplars to potential cluster members, indicating how appropriate that candidate would be as an exemplar.
- *Responsability*: Message sent from cluster members to candidate exemplars, indicating how well-suited the data point would be as a member of the candidate exemplar's cluster.

The *net-similarity* is a score, defined as the sum of the total *availability* and the total *responsability* and it is the objective function that affinity propagation tries to maximize.

Affinity propagation iteratively computes responsibilities and availabilities. The algorithm terminates if decisions for the exemplars

and the cluster boundaries are unchanged for convits iterations, or if maxits iterations are reached.

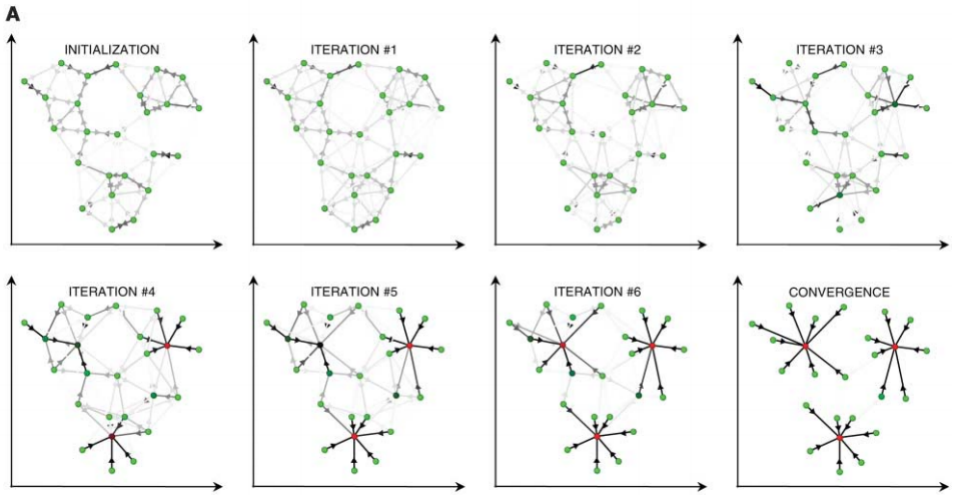

Figure 3.19: An example of the evolution during iteration of the Affinity Propagation algorithm. Red points are the exemplar found. The arrow show the messages exchange.

This kind of clustering was chosen, first, for its capability to automatic find the number of cluster and then for its different approach compared to the K-Means clustering. In fact, as shown above, affinity propagation doesn't realize a real space partitionin, but it makes compete the sample, fusing a distance-based clustering method, with a competitive unsupervised method. The hope was that such algorithm was able to find hidden similarities.

3.5 The optimization problem (G)

The optimization was performed just one time. The loop described in figure 3.1 is closed just once (point G).

In the section 3.3 were introduced the fact that each subgraph enumerated would be considered significative for a further analysis only if respecting two constraints:

- $f_{original}(S_k) \leq U$
- $|zScore(S_k)| \geq Z$

A real problem was the choice of the best value for U and Z. Since both size-3 and size-4 subgraphs were searched, a set of four parameters estimation was required: two for size-3 subgraphs, i.e. U_3 and Z_3, two for size-4 subgraphs, i.e. U_4 and Z_4.

The optimization of these parameters was based on the quality of the classification of the leads, and so False Negatives and False Positives, in function of $\{U, Z_3, U_4, Z_4\}$ were minimized.

False Negatives and False Positives were computed changing incresing consecutively each parameter of 0.5. Each parameter started from 0.5. In figures 3.20 and 3.21 the FN and FP trend is displayed. Each iteration corresponds to a combination of the four parameters.

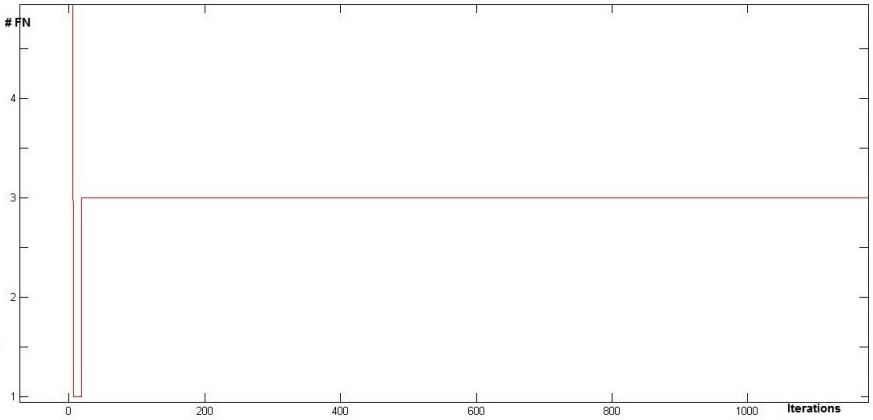

Figure 3.20: False negative trend in patient 14

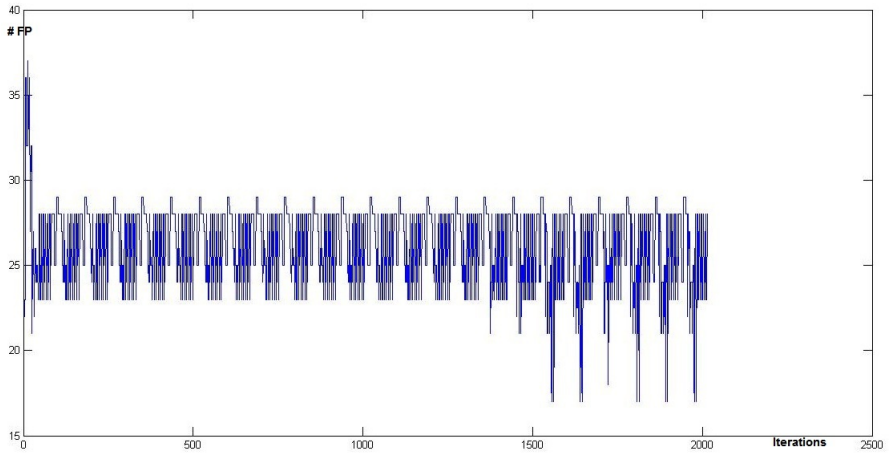

Figure 3.21: False positive trend in patient 14. It present a large number of local minima.

Considering the goal of the classification, is more important to have no False Negative. In fact having false negative rate equal to zero, means that the neurologist can consider only the cluster labeled as epileptogenic and anlyzing only the leads owning to that cluster, reducing the analysis even from one hundred leads to fifteen or ten!

The solving of the problem was in two step.

1. Search all the False Negative minimum
2. Looking for the False Positive minimum only in the range where the false negative rate is minimum.

The optimization was performed using 4 FCD (Focal Cortical Dysplasia) patients (Pt2, Pt3, Pt10, Pt13) chosen by chance from the totality of the FCD patients.

Chapter 4

Results

In this work were considered SEEG multichannel recordings of 3 minutes of interictal activity selected by neurologists from subjects with a seizure-free outocome after cortical ablation surgery (Engel Class I[1]). Signal windows were selected according to their quality and the absence of relevant artifact and labeled as EZ or NEZ by a neurologist. The data was recorded during the invasive presurgical work-up at the Epilepsy Surgery center of Niguarda Hospital in Milan. Subjects were monitored for up to several days in order to characterize their seizures and assess their candidacy for surgery. Recordings were collected from 18 subjects with partial drug-resistant epilpepsy (15 FDC, 1 PT, 2 PMG). Raw signals were sampled at 1000 Hz and, after low pass filtering at 120 Hz to avoid aliasing, downsampled at 250 Hz. The number of channels included in each record ranged from 30 to 90. All the derivations considered was bipolar, leading to a more localized study of the neuronal activity. In order to protect the privacy of the subjects, all health information in the original files was removed.

Results of the optimization problem (section 3.5) are summarized

[1] Jerome Engel proposed a scheme, made by four classes, to classify postoperative outcome for epilepsy surgery, which has become a standard when reporting results in medical literature [43].

in the following table:

Par	Value
U_3	1.5
Z_3	3
U_4	0.5
Z_4	0.5

Table 4.1: Optimum parameters obtained as result of the optimization problem explained in 3.5. They represent the cut-off of Frequencies and Z-Score.

Those parameters were used as thresholds for the selection of the most significative subgraphs.

In the next are showed different clustering settings with the same four patients (Pt2, Pt3, Pt10, Pt13) used for the optimization problem, in order to choose the best configuration.

Roles Fingerprints Matrix related to leads of each of the four patients were clusterized with the two methods described in section 3.4: 18 Roles Fingerprint Matrixes were computed, with different combination of dimensions of subgraphs enumerated and randomization modalities:

1. Size-4 subraphs with all three randomness models
2. Size-4 subraphs with Local random and Global random
3. Size-4 subraphs with Local and NoRegard
4. Size-4 subraphs with Global and NoRegard
5. Size-4 subraphs with Local alone
6. Size-4 subraphs with Global alone
7. Size-4 subraphs with NoRegard alone
8. Size-3 subraphs with all three randomness models
9. Size-3 subraphs with Local random and Global random

10. Size-3 subraphs with Local and NoRegard
11. Size-3 subraphs with Global and NoRegard
12. Size-3 subraphs with Local alone
13. Size-3 subraphs with Global alone
14. Size-3 subraphs with NoRegard alone
15. Size-3 and 4 subgraphs with all three randomness models.
16. Size-3 and 4 Local Randomness.
17. Size-3 and 4 Global Randomness.
18. Size 3 and 4 No-Regard Randomness.

In the followinf figure the K-Means cluster overall numbers for the Pt2, Pt3, Pt10, Pt13 and for different numbers of clusters:

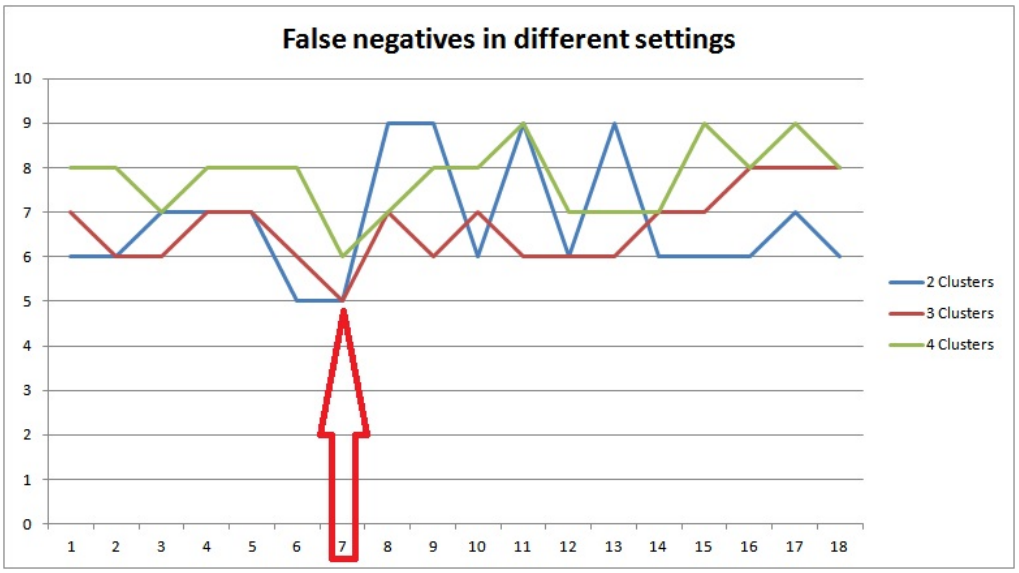

Figure 4.1: False Negatives for each combination in above list and varying the number of clusters in K-means clustering. Combination 7 gave the best performance.

The same study was performed used the Affinity Propagation clustering, with the difference that for the Affinity Propagation the number of cluster is automatically chosen.

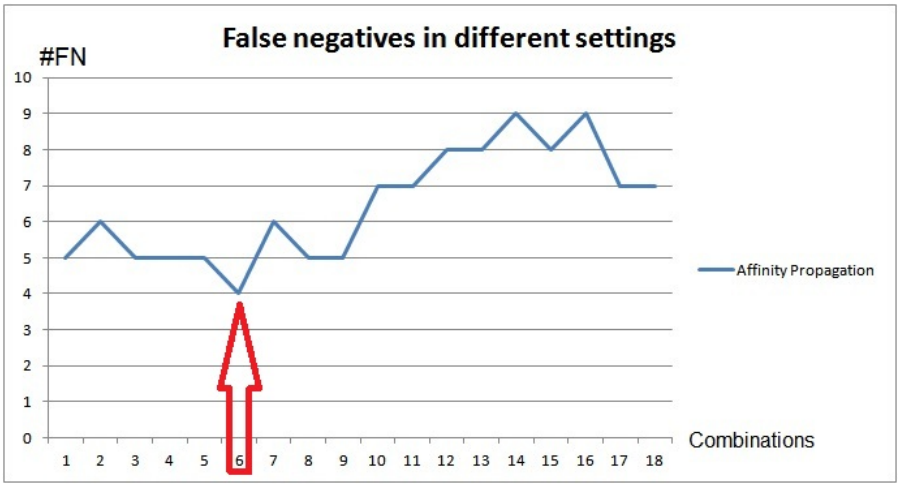

Figure 4.2: False Negatives for each combination in above list with Affinity Propagation clustering. Combination 6 gave the best performance.

The best combination, and then the one chosen, was that with the least overall number of False Negative on the four patients (Pt2, Pt3, Pt10, Pt13). So for the K-Means clustering was chosen the combination number 7, Size-4 subraphs with No Regard model. It was chosen because there is a minimum also using 4 clusters. Using four clusters is better than three, becuase there should be a lesser number of False Positive. For Affinity Propagation was selected the combination number 6, Size-4 subraphs with Global alone. Affinity Propagations always computed three clusters. For further patients this number could change.

In the table 4.2 the setting for the two clusterings is summarized.

$U_3 = 1.5$ $Z_3 = 3$ $U_4 = 0.5$ $Z_4 = 0.5$	
Size-4 Subgraphs	
K-Means	*Affinity Propag.*
Model: *No regard*	Model: *Global*
$N.Cluster = 4$	$Preference = min(s)$

Table 4.2: Recap of the parameters used for K-Means clustering and Affnity Propagation

Then, using the setting evalutaed with the study of false negative, in order to obtain the least number of them, classification algorithms were performed on the remaining 14 patients. In tables 4.4 and 4.4 are shown the performance in absolute number and with percentage values (*FNR*, *FPR*, *Accuracy*).

Patients	Pathology	Leads	EZ	KM FN	KM FP	AP FN	AP FP
Pt1	Taylor	84	4	0	15	0	57
Pt4	Taylor	66	4	0	22	0	60
Pt5	Taylor	38	2	0	10	0	34
Pt7	Taylor	52	6	0	14	0	12
Pt11	Taylor	65	2	0	12	0	25
Pt12	Taylor	81	5	0	9	0	59
Pt14	Taylor	72	7	4	25	4	29
Pt15	Taylor	64	4	2	14	0	58
Pt16	Taylor	56	3	1	12	0	29
Pt17	Taylor	45	4	0	11	0	9
Pt18	Taylor	62	2	0	22	0	58
Pt6	Post Tr.	80	7	1	16	0	71
Pt8	PMG	69	12	4	14	5	22
Pt9	PMG	73	8	1	13	3	14
Pt2	Taylor	79	6	1	10	1	28
Pt3	Taylor	33	3	0	8	0	8
Pt10	Taylor	69	5	0	8	0	30
Pt13	Taylor	71	6	4	15	3	46

Table 4.3: The table shows the overall automatic classification performances. *Leads* column is the number of analyzed leads. *EZ* is the number of leads labeled as Epileptogenic. *KM FN* and *KM FP* show the number of false negatives and false positives obtained with K-Means clustering. *AP FN* and *AP FP* show the number of false negatives and false positives obtained with Affinity Propagation.

Patient	Pathology	KM FNR	KM FPR	KM Acc.	AP FNR	AP FPR	AP Acc.
Pt1	Taylor	0%	19 %	82%	0%	71%	31%
Pt4	Taylor	0%	35 %	66%	0%	97%	8%
Pt5	Taylor	0%	28 %	73%	0%	94%	8%
Pt7	Taylor	0%	30 %	73%	0%	26%	76%
Pt11	Taylor	0%	19 %	81%	0%	40%	61%
Pt12	Taylor	0%	12 %	89%	0%	78%	26%
Pt14	Taylor	67%	38 %	59%	67%	45%	54%
Pt15	Taylor	67%	23 %	75%	0%	97%	8%
Pt16	Taylor	50%	23 %	76%	0%	55%	47%
Pt17	Taylor	0%	27 %	75%	0%	22%	80%
Pt18	Taylor	0%	37 %	64%	0%	97%	5%
Pt6	Post Tr.	17%	22 %	78%	0%	97%	10%
Pt8	PMG	36%	25 %	74%	45%	39%	60%
Pt9	PMG	14%	20 %	81%	43%	22%	76%
Pt2	Taylor	20%	14 %	86%	20%	38%	63%
Pt3	Taylor	0%	27 %	75%	0%	27%	75%
Pt10	Taylor	0%	13 %	88%	0%	47%	56%
Pt13	Taylor	80%	23 %	73%	60%	71%	30%

Table 4.4: False Negative Rate, False Positive Rate and Accuracy of the automatic method for all the patients.

Finally, in the following charts are summarized the performances of the two clusterings.

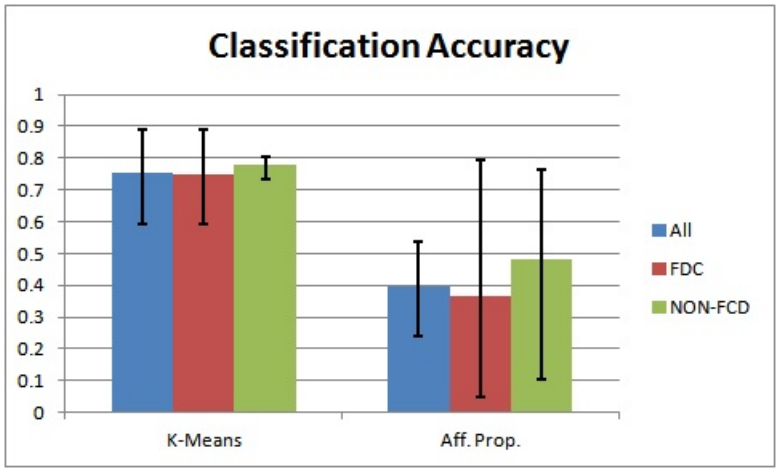

Figure 4.3: Accuracy, mean, maximum and minimum, of the two clustering methods, considering all the patients (blue), only those affected by Focal Cortical Dysplasia (red) and those with non-FCD (green). These results don't consider the four patients used for the optimization (Pt2, Pt3, Pt10, Pt13).

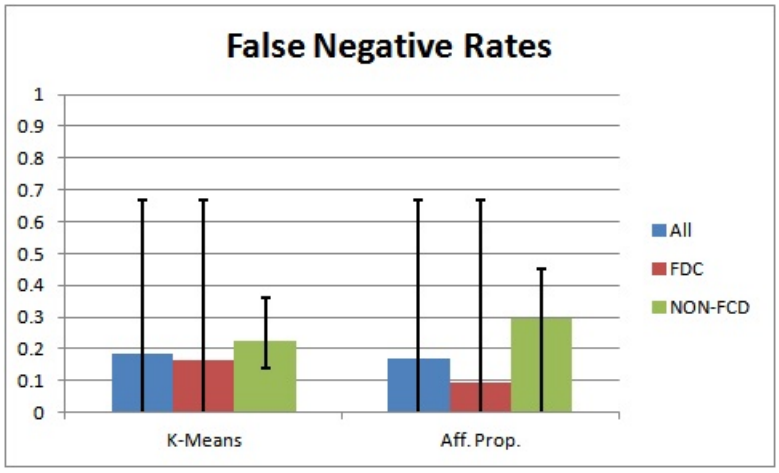

Figure 4.4: False Negative Rates, mean, maximum and minimum, of the two clustering methods, considering all the patients (blue), only those affected by Focal Cortical Dysplasia (red) and those with non-FCD (green). These results don't consider the four patients used for the optimization (Pt2, Pt3, Pt10, Pt13).

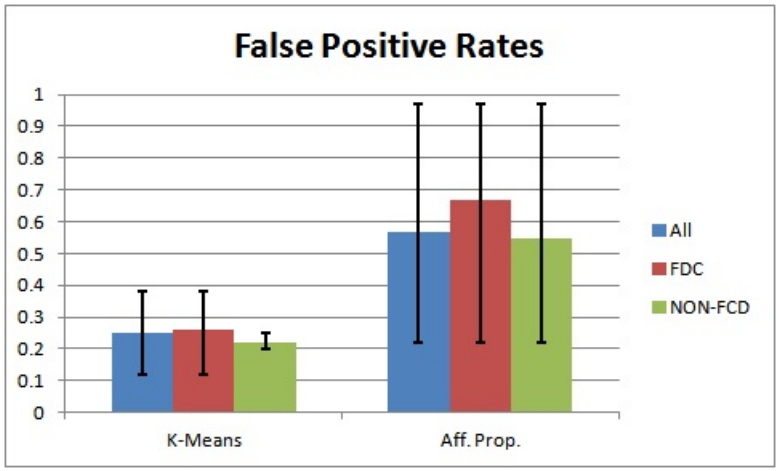

Figure 4.5: False Positive Rates, mean, maximum and minimum, of the two clustering methods, considering all the patients (blue), only those affected by Focal Cortical Dysplasia (red) and those with non-FCD (green). These results don't consider the four patients used for the optimization (Pt2, Pt3, Pt10, Pt13).

The F-Score was performed only on the overall classification.

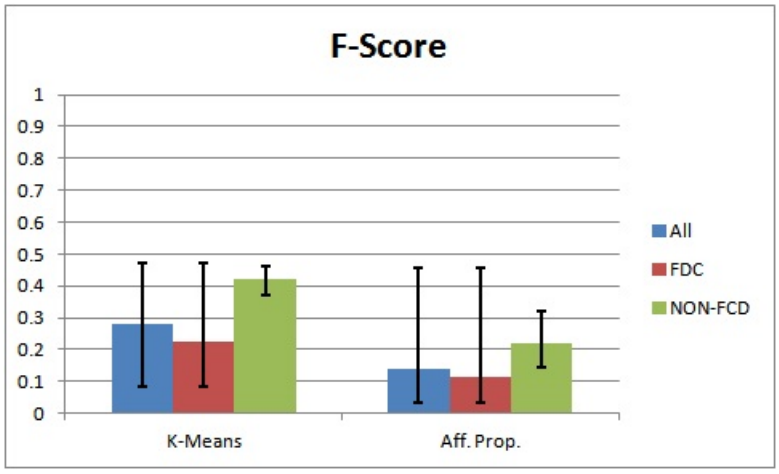

Figure 4.6: F-Score, mean, maximum and minimum, of the two clustering methods, considering all the patients (blue), only those affected by Focal Cortical Dysplasia (red) and those with non-FCD (green). These results don't consider the four patients used for the optimization (Pt2, Pt3, Pt10, Pt13).

Chi-squared test was performed on the overall success and failure

of the algorithm. The obtained value was $\chi^2 = 241.2$ and the critical value tables is $\chi^2_{crit} = 10.83$. So the null hyphotesis was rejected.

Chapter 5

Discussions and Conclusions

5.1 Discussions and Conclusions

Partial epilepsies are in the 40% of the cases drug-resistant. The only treatment available in order to lead those epileptic subjects to a total healing is the ablation surgery of the epileptogenic cortical area (EZ), which must be accurately localized during the pre-surgical planning. Localizing EZ cortex is a very critical task, because the goal is the total seizure-free outcome with the minor cortical damage. In some cases, when the EZ localization is particularly hard, the electric activity of the brain is inspected with the invasive insertion of electrodes within the brain, in order to record depth-EEG for some weeks. The amount of signal that neurologists have to deeply visual inspect is huge, making the EZ localization a very time consuming activity.

The objective of this thesis was the implementation of an automatic classifer able to achieve an accurate classification of the interictal SEEG signal with the purpose of helping clinician in the EZ identification.

SEEG signals of 18 drug-resistant partial epileptic patients with seizure-free outcome (Engel Class I) were analyzed. Dataset of each

patients were composed by 3 minutes of signal recorded by a variable number of channels (from 30 to 90), and it is splitted in 36 epochs. From each epoch a connectivity matrix was computed.

Then connectivity matrixes underwent the network analysis, leading to Roles Fingerprint Matrixes (one for each patient) as output. Then Roles Fingerprint Matrixes, were each row was a SEEG lead, were used as input for two clustering techniques (K-Means and Affinity Propagation). Finally the classification was performed providing just one EZ lead (labeled by neurologist) to the algorithm in order to localize the EZ cluster, classifying all the leads in it as EZ. The runtime for each patient is about 6 hours. Network analysis script was implemented in C++ and compiled on a linux based operative system. Role Fingerprint generation and clustering were implemented with .NET libraries and runned on windows 7.

Methods choice Analysing SEEG signals with the purpose of localizing the epileptogenic zone is a very critical task. Each kind of epilepsy shows different typical signal events, and it's impossible to find a common "epileptic pattern". Plus, SEEG signal changes a lot according to the brain region where the leads are inserted within. For example, a signal recorded by a lead in a healty primary motor cortex, sometimes shows very fast fluctuation, which are very similar to those showed by the onset signal. The human eye can recognize that difference, but it's impossibile for a computer. For these reasons the approach chosen, with the computation of the Roles, tried to go beyond the mere signal processing. In fact, the purpose was to find different behaviours of each channel of the SEEG respectively to other channels. The performed network analysis accomplished this objective, studying all the channels together and then assigning to each of them a series of characterizing values (Roles). In order o classify Roles, an unsupervised method was prefered for two main reasons:

- The classification must be patient-custom, due to the great difference between each case of epilepsy. The dataset related to each patient, was to poor for a division in a training, validation and testing set, which are essential for the use of a supervised method.
- The goal was the leads classification with the least a-priori information provided by clinicians.

Cluster analysis on the 18 patients shows that in some cases, especially in the Focal Cortical Dysplasia, it's possibile to find a real epileptogenic class among the dataset. Anyway it is not always possibile, maybe due to the reasons explained above, or maybe due to the implemented method. When an EZ lead is classified as NEZ, meaning that it is in NEZ cluster, it's arguable that its Roles Fingerprint is too different from the one represented in the EZ cluster, suggesting two things:

- The need of two (or even more) EZ clusters.
- A failure in the classification method.

Classification performances The difference in the classification between the two clustering methods was checked with the Chi-Square test. Since the obtained value was greater than the tabled critical value, the null hypothesis, that the performance of the two classifier was similar, must be rejected. Performances obtained, considering the number of False Negative, are better considering only the size-4 subgraphs. The reason is that the size-3 subgraphs cannot really express the behaviour of each node in the network.

- *Affinity Propagation (AP):* Accuracy Chart (Chart 4.3) shows that the Affinity Propagation Clustering doesn't fit the problem (overall accuracy of about 39%). In fact, even if Affinity Propagation has a little number of False Negative (Chart 4.4),

the classification obtained with AP has very low accuracy due to a very high False Positive Rate (Chart 4.5). This high number of False Positives leads to a very imbalanced classification, in fact the F-Score related to AP method is very small.

- *K-Means (KM):* K-Means clustering (KM) works quite well with an overall accuracy of 75,5% (without considering Pt2, Pt3, Pt10, pt13). Anyway, as already explained, the problem was focused on obtaining the fewest possibile number of False Negative. In fact, the overall FNR (always not considering Pt2, Pt3, Pt10, pt13) is 18.5% and the mean F-score show an imbalanced classification performance, according to the type of optimization performed. Performances were also computed dividing the FCD cases from Post Traumatic and Polymicrogyria, because FDC epileptogenic zone is usually easier to find. As showed in Charts 4.3, 4.4, 4.5, performances between the two kind of pathologies are very similar. But considering Post Traumatic epilepsies and PMG was impossible to obtain a FNR equal to zero (tables 4.3 and 4.4), which should be the ultimate goal of a EZ classifier. Talking about results concernings the FCD, they are very good except for three patients (Pt14, Pt15, Pt16) where there is a quite large number of False Negatives. The first reflection about the performances described is that the computation of the False Negative was performed on the basis of the labels of the leads provided by neurologist. There is chance that a neurologist misclassified a lead, even if this is a very rare event, especially in FCD cases. Another critical point is discussed in the following paragraph.

Method optimality *Performances obtained are the best possible using such input data?* The answer is that there are a lot of critical aspects which could influence results.

- There isn't any evidence that the h^2 index is the most suitable

measure for a connectivity estimation. h^2 index uses the signal without selecting the frequencies to study. Since epileptic phenoma are often bound to high frequency, a selective connectivity index that works only on SEEG gamma (and delta) band, may improve the classification performances.

- In some other works [2] the threshold used on h^2index to define the presence or not of a connection between two elements, it's different. In fact the other criterion is to use the mean h^2value, computed on the whole connectivity matrix..
- The most critical task of this work is optimization of the parameters set $\{U_3, Z_3, U_4, Z_4\}$. First, the upgrading step of the parameters during the optimization phase was quite high, but the choice was made according to computational constraints. Plus the dataset was very limited. To have a very profitable optimization a larger dataset is required, maybe with a greater number of non-FCD patients. In fact the parameters obtained optimizing four FCD patients are used also for non-FCD patients, surely introducing a bias in the performance.

Conclusion The outcome of this work is a quite good classification method for SEEG signals in order to identify the Epileptogenic Zone among the SEEG leads. Even if the dataset used was too poor to lead a ultimate conclusion, the method seems to be not sufficiently reliable for a stand-alone clinical use. Anyway it's a big step forward on the path to a performant automatic method for the EZ localization. It's the first time that a method shows such quite good performances in the SEEG signals classification, able to handle different epilepsy types. The method proposed can be used synergistically with clinicians, in order to decrese the number of signals that they have to visual analyze.

5.2 Future Work

The developed method shows quite good classification capacities but with a great bias in non-FCD cases. The work described is just a starting point for several possible further developments:

- The use of a more extended SEEG signal window. Especially could be nice collecting SEEG interictal section day-far recorded, and analyzing roles trend of each single node in time. Anyway, of course, the most interesting signal section would be the onset one, in order to compare this work with the other that took into consideridation just such that part of the signal. Another trial could be done analyzing the seizure signal, but it may be too much noisy for an acceptable outcome.

- Size-k subgraphs were considered only with $k = 3$ and $k = 4$. The analysis with $k \geq 5$ may improve the classification power of the algorithm. In fact in this work size-3 subgrahs showed worse performances than the size-4 subgraphs. The real issue is that searching for significantive subgraphs with more than 5 nodes require a long time and a powered-up hardware configuration. Plus the role computation script must be written with a paralleling computation conception because the runtime with larger subgraph increases factorially with their size.

- In this work the Role Fingerprint Matrix were analyzed with a clustering method. A lot of other different approach could a lead to very satisfactory results. For instance, role fingerprint could be designed with a transition state model and then studied with a HMM[1] method. In this case the critical aspect could

[1] A Hidden Markov Model (HMM) is a Markov chain for which the state is only partially observable. In other words, observations are related to the state of the system, but they are typically insufficient to precisely determine the state. Several well-known algorithms for hidden Markov models exist. For example, given a sequence of observations, the Viterbi algorithm will compute the most-likely corresponding sequence of states, the forward algorithm will compute the probability of the sequence of observations, and the Baum–Welch algorithm will

be the definition of the alphabet to use and its length. Role Fingerprint seems also to fit on a possibile RM-ANOVA[2] analysis, because with it, it's possibile to find the different distribution behaviour in time, fetching the different trend of evolution of the activity of each signle recording node.

- Adding to the described method a Graphic User Interface (GUI) could boost its attractiveness from the point of view of the clinicians. Building a 3D Slicer[3] module that fuse the information provided by the classificator with the information extracted by bioimages could become a very reliable instrument for the preoperative planning phase.

estimate the starting probabilities, the transition function, and the observation function of a hidden Markov model.

[2]One-Way ANOVA looks at differences between different samples exposed to different manipulations (or different samples that may come from different groups) within a single factor. RM-ANOVA is a techinque that can take into account a multichannel dataset.

[3]3D Slicer (Slicer) is a free, open source software package for image analysis and scientific visualization. Slicer is used in a variety of medical applications

Appendix A

Appendix

GRAPHS

Some basic familiarity with graph-theoretic terminology must be provided. For a given graph $G = (V, E)$, V is the set of *Vertices* and E is the set of *Edges.* *Vertices* are the nodes, particularly in this work they represent the SEEG electrodes leads. The *edges* are the links between vertices (see figure A.1) and they represent the functional connectivity between leads. Let $n := |V|$ ($length(V)$) and assume that all vertices in V are uniquely labeled by the integers $1, ..., n$. To abbreviate that the label of a vertex u is larger than that of a vertex v, will be written "$u > v$". In order to simplify the presentation, *edges* in $G = (V, E)$ are always identified using set notation, regardless of whether the graph is directed or undirected. In the case that G is directed (figure 3.6) and contains the edges (u, v) and (v, u) for two vertices u and v, these edges become a single *bidirectional edge* $\{u, v\}$ (in this notation). For a set $V' \subseteq V$ of vertices, its open neighborhood $N(V')$ is the set of all vertices from $V \setminus V'$ (\stands for the difference between two sets) which are adjacent to at least one vertex in V'. For a vertex $v \in V \setminus V'$, its exclusive neighborhood with respect to V', denoted $N_{excl}(v, V')$,

consists of all vertices neighboring v that do not belong to $V' \cup N(V')$. A connected subgraph that is induced by a vertex set of cardinality k is called *size-k subgraph*. For a given integer k, the set of all size-k subgraphs in G can be partitioned into sets $S_k^i(G)$ called subgraph classes, where two size-k subgraphs belong to the same subgraph class if and only if they are *isomorphic,* that is, if and only if they are topologically equivalent (see paragraph A).

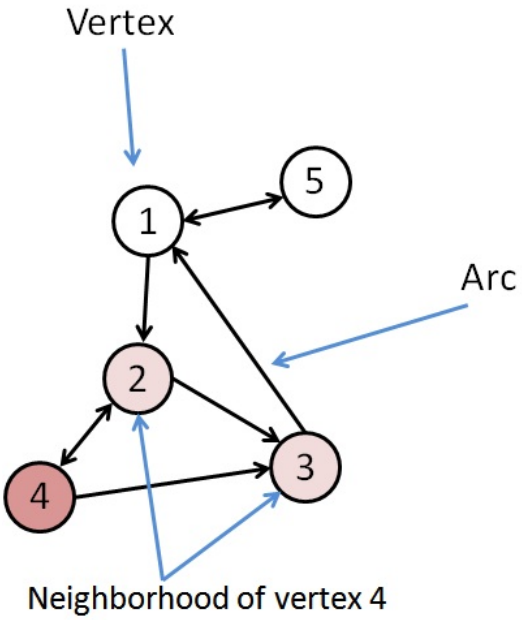

Figure A.1: Notation about graphs

Isomorphic subgraphs

In abstract algebra, an isomorphism is a bijective[1] homomorphism[2]. Two mathematical structures are said to be isomorphic if there is

[1] In mathematics, a bijection (or bijective function or one-to-one correspondence) is a function giving an exact pairing of the elements of two sets. Every element of one set is paired with exactly one element of the other set, and every element of the other set is paired with exactly one element of the first set. There are no unpaired elements. In formal mathematical terms, a bijective function $f : X \to Y$ is a one to one and onto mapping of a set X to a set Y.

[2] In abstract algebra, a homomorphism is a structure-preserving map between two algebraic structures

an isomorphism between them.

In the graph theory two graphs $G_1 = (V_1,\, E_1)$ and $G_2 = (V_2,\, E_2)$ are defined isomorphic if there is a biunique correspondence between them:

$$\varphi : V(G_1) \to V(G_2) \;:\; (u, v) \in E(G_1) \Longleftrightarrow (\varphi(u), \varphi(v)) \in E(G_2) \tag{A.1}$$

The mathematical formalization in A.1 can be translate in: *two graphs are isomorphic if only their representation is different, but they are the same structure. To be more precise, two graphs $G_1$and $G_2$are isomorphic if there a biunique correspondence between vertexes of $G_1$and vertexes of $G_2$and if exists a biunique correspondence between the edges of $G_1$and those of G_2which preserve the same incidence rule. A vertex and an edge of G_1 have a corresponding vertex and edge in G_2*. Two isomorphic graphs are identified with the following notation: $G_1 \cong G_2$.

In the figures 3.10 and A.2 are showed some example of isomorphic graphs in order to clarify the meaning of that concept. A careful reader may note that a possible informal definition for graph isomorphism could be that two graphs are isomorphic if they are equal except for a *permutation of the vertex labels.*

The figure A.2 highlights that two graphs are isomorphic if the picture of one can be led to fit with the other one without breaking the links (Edges) connecting the vertices.

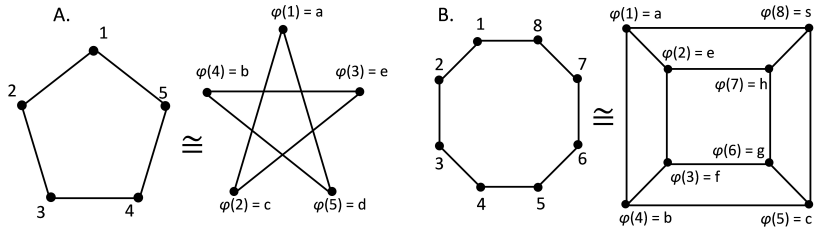

Figure A.2: Two examples of isomorphic graphs. *A*: 5-size graphs. *B*: 8-size graphs.

Isomorphic graphs have the following properties:

1. Vertexes number $|V(G)|$ doesn't change after an isomorphic transformation: isomorphism is a biunique correspondence of the vertexes sets of the graphs and then the cardinality of the two array $V(G_1)$ and $V(G_2)$ must be the same.

2. Two isomorphic graphs have the same number of edges: an isomorphic tranformation sends adjacent vertexes to adjacent vertexes and it is biunique, so also the number of links between vertexes doesn't change.

3. Isomorphic graphs have the same vertex degree[3] distribution: if G owns *k' d-degree vertexes*, each isomorphic graph has exactlyk' *d-degree vertexes*. In fact if $v \in V(G_1)$is adjacent to $u_1, ..., u_k \in V(G_1)$, $\varphi(v) \in v(G_2)$is adjacent to $\varphi(u_1), ..., \varphi(u_k) \in V(G_2)$ and it cannot be adjacent to any other vertex in order to not break the biunique correspondence.

Isomorphisms from an object to itself is called *automorphism*. To be more specific, a graph automorphism is when there is vertex mapping that preserves vertex and edge connectivity (e.g. an isomorphism of the vertices onto the same graph). In example in figure A.3.

[3] *Vertex degree*: sum of the inwards connection and the outwards connection of a vertex in a directed graph. In an undirected graph it's just the sum of connection of a vertex.

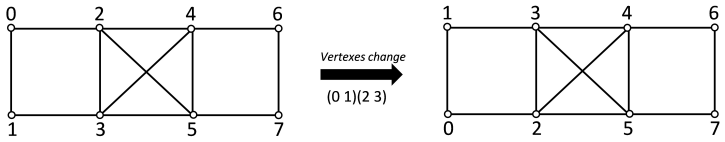

Figure A.3: An example of automorphism. Using a one to one matching criterion the two graphs will be marked as different, even if they are the same graph!

In order to accomplish a motif detection of a large network is mandatory to indentify all the isomorphic size-k subgraphs and collect them in classes. The reason is that the interest is focused on the relation between nodes and not on the actual path of the information flow. Establish that two subgraphs are isomorphic is a NP-complete[4] problem (thanks to biunique properties), and so it's possible to build a polynomial algorithm able to carry out the task. There some different algorithms able to efficiently detect isomorphic subgraphs in a network. In this work was used Nauty Algorithm [38], which is the fastest one [40].

Isomorphism Detection

In order to make the reader understand how the algorithm works, will be given some formal definitions. Then the concept of Search Tree will be defined and will be provided an explaination on how it enables computation of automorphism groups and canonical forms [44].

- A *Colouring* of V (set of vertices $V = \{1, 2, ..., n\}$) is a surjective[5] function π from V onto $\{1, 2, ..., k\}$ for some k. The

[4] NP-complete is a subset of NP class, the set of all decision problems whose solutions can be verified in polynomial time; NP may be equivalently defined as the set of decision problems that can be solved in polynomial time on a nondeterministic Turing machine. A problem p in NP is also NP-complete if every other problem in NP can be transformed into p in polynomial time.

[5] In mathematics, a function f from a set X to a set Y is surjective (or onto), or a surjection, if every element y in Y has a corresponding element x in X given by $f(x) = y$. Multiple elements of X might be turned into the same element of Y by applying f.

number of colours, i.e. k, is denoted by $|\pi|$. A cell of π is the set of vertices with some given colour, that is, $\pi^{-1}(j)$ for some j with $1 \leq j \leq |\pi|$. A discrete colouring is a colouring in which each cell is a singleton, in which case $|\pi| = n$. Note that a discrete colouring is a permutation of V . A pair (G, π), where π is a colouring of G, is called a *coloured graph*.

- A *canonical isomorph function* assigns to every graph G an isomorph $L(G)$ such that whenever a graph H is isomorphic to G it has $L(H) = L(G)$. $L(G)$ is called the canonical isomorph of G. From this concept derives the process of *Canonical Labeling:* given a class of objects one can choose one member of each isomorphism class and call it the canonical member of the class. The process of finding the canonical member of the isomorphism class containing a given object is called canonical labeling. Two labeled objects which are isomorphic become identical when they are canonically labeled. Since identity of objects is usually far easier to check than isomorphism, canonical labeling is the preferred method of sorting a collection of objects into isomorphism classes. A possible definition of the canonical member of an isomorphism class would be the member which maximises some linear representation (such as a list of edges). Formalizing, $L : \Theta \times \Pi$, where $G \in \Theta$and $\pi \in \Pi$.

- The *Search Tree* $T(G)$ is a rooted tree created for each subgraph, whose nodes correspond to sequences of vertices, with the empty sequence at the root of the tree. The sequences become longer moving down through the tree. Each sequence corresponds to a colouring of the graph obtained by giving the vertices in the sequence unique colours then inferring in a controlled fashion a colouring of the other vertices. Leaves of the tree correspond to sequences for which the derived colouring is discrete. The *Refinament function* defined in the following

point is the core of the *Search Tree Build up* procedure. It specifies the colouring that corresponds to a sequence.

- A key concept used by Nauty is partition refinement (*partition = colouring*). *An equitable partition is one where every two vertices of the same colour are adjacent to the same number of vertices of each colour.* Refinement of a partition means to subdivide its cells. Given a partition (colouring) π, there is a unique equitable partition that is a refinement of π and has the least number of colours. Figure A.4 shows the steps which lead from an initial colouring to the equitable partition. The black arrows indicate vertices having a number of neighbours in a reference cell which is different from that of other vertices in their cell. The *refinement function* $R(G, \pi, \alpha)$ is clearly described in Algorithm A.1. In practice most of the execution time of the whole algorithm is devoted to refining colourings, so its implementation is critical. While the function R defined above works well for many graphs, there are difficult classes for which it does not adequately separate inequivalent vertices. Regular graphs are the simplest example, since the colouring with only one colour is equitable. Nauty provides a small library of stronger partitioning functions, some of them designed for particular classes of difficult graphs.

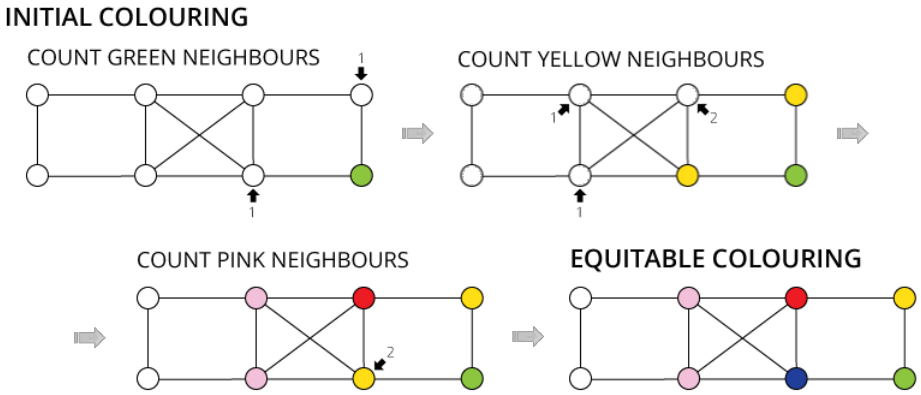

Figure A.4: Steps of the Refinement Algorithm, which lead to a consecutive partitioning of a graph assigning different colorus to similar neighborhood. Each iteration of the algorithm is a node in the Search Tree.

Algorithm A.1 REFINEMENT FUNCTION

Input: π is the input colouring and α is a sequence of some cells of π.
Output: the final value of π is the output colouring.

```
01 while α is not empty and π is not discrete do
02     Remove some element W from α.
03     for each cell X of π do
04         Let X_1,...,X_k be the fragments of X distinguished according
                        to the number of edges from each vertex to W.
05         Replace X by X_1,...,X_k in π.
06         if X ∈ α then
07                 Replace X by X_1,...,X_k in α.
08         else
09                 Add all but one of the largest of X_1,...,X_k to α.
10         end
11     end
12 end
```

Nauty algorithm starts by forming the equitable refinement of the unit partition, thereby extracting all of the initial degree information. Then the Refinement Function iterates and, adding a level in *Search Tree* after each colour refinement, it systematically explores the space of equitable ordered partitions and at the same time it

builds the Tree.

The terminal nodes of the search tree are nodes with no outgoing arcs. These terminal nodes correspond to discrete ordered partitions of ther given Graph, i.e. all it's possible equitable topologic forms. Given a discrete ordered partition $\pi = (V_1, V_2, ..., V_m)$ (a leaf of the Search Tree), let $\sigma_\pi \in \Sigma_n$ to be a permutation among the all possible permutarions such that $i^{(\sigma_\pi)} = j$ if V_j contains i. For example, if $\pi =$ (1|9|3|7|8|6|4|2|5), thenσ_π maps $1 \to 1, 9 \to 2, 3 \to 3\ , 7 \to 4, 8 \to 5$, and so on. To each terminal node it is possible to associate the isomorph $G^{(\sigma_\pi)}$ of G. The Canonical Isomorph Function is defined to be

$$L_M(G) = \max_{\Lambda} \left\{ G^{(\sigma_\pi)} \ : \ (\pi; \underset{\sim}{u}) \, is \, a \, leaf \, of \, T(G) \right\}$$

where $\Lambda$is the set of the numbers of substitutions for the each σ_π permutation. Anyway the canonical label can be chosen also imposing different criteria. The one described fit well with the analysis of small subgraphs (k=3 and k=4).

The Canonical Function is used to canonize its isomorphic subgraphs in order to have only a class for that isomorphic family.

Here a summering of the method: the nodes of the tree correspond to partitions (colourings). The root of the tree corresponds to the initial colouring, refined. If a node corresponds to a discrete partition (each vertex with a different colour), it has no children and it is a leaf. Otherwise a chosen colour used more than once (the target cell), individualize one of those vertices by giving it a new unique colour, and refine to get a child. Each leaf lists the vertices in some order (since colours have a predefined order), so it corresponds to a labelling of the graph. *If two leaves give the same labelled graph, there is an automorphsim.* If an order on labelled graphs is defined,

such as lexicographic order [6], then the greatest labelled graph corresponding to a leaf is a canonical graph. However the tree can be much too large to generate completely. It will be pruned by means of node invariants. A node invariant is a value$\Phi(\nu)$ attached to each node ν in the tree that depends only on the combinatorial properties of ν and its ancestors in the search tree (not on the labelling of the graph). Node invariants, together with automorphisms, allow us to remove parts of the search tree without generating them.

- If l_1, l_2 are nodes at the same level in the search tree and $\Phi(l_1) < \Phi(l_2)$, then no canonical labelling is descended from l_1.
- If l_1, l_2 are nodes at the same level in the search tree and $\Phi(l_1) \neq \Phi(l_2)$, then no labelled graph descended from $\nu 1$ is the same as one descended from l_2.
- If l_1, l_2 are nodes with $l_2 = (l_1)^g$ for an automorphism g, then g maps the subtree descended from l_1 onto the subtree descended from l_2.

Pruning the Tree is very important to reduce the computational time and complexity of it and it's the reason that Nauty Algorithm is much better than a full enumeration of the all permutation of each graph.

Nauty Algorithm is based on three main ideas:

1. Using, iteratively, degree information of vertexes.
2. Building a search tree examining choices non determined by degree information.
3. Pruning the tree using graph automorphirsm and nodes invariants.

[6] In mathematics, the l*exicographic* or *lexicographical order* (also known as lexical order, dictionary order, alphabetical order or lexicographic(al) product) is a generalization of the way the alphabetical order of words is based on the alphabetical order of their component letters

The Tree is an instrument to assign a label, i.e. a class to each subgraph found in the whole network. The strenght of the Tree is that its building process is very fast and during that a lot of useless information is discharged (e.g automorphism). Then for each subgraph there is a sort of matching function (Canonical Labelling), where each possibile form of the a subgraph is matched with its correspondence label. So it's possibile to split up the subgraphs set in a class set just with a one to one matching, faster than any other kind of coupling.

Here a complete nauty user guide [39]. Instead for a deeper mathematical argumentation the reader can read the original McKay's document about Nauty algorithm [38].

A very simple example for a further clarification of the algorirhm workflow is given considering the following size-9 graph:

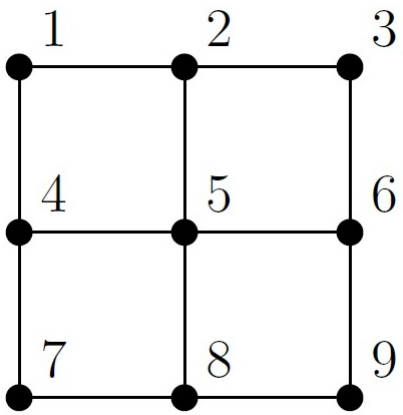

Figure A.5: A size-9 graph *G=(V,E)* where $|V| = 9$ and $|E| = 12$.

From that graph, using iteratively the refinement function its related Search Tree is built up:

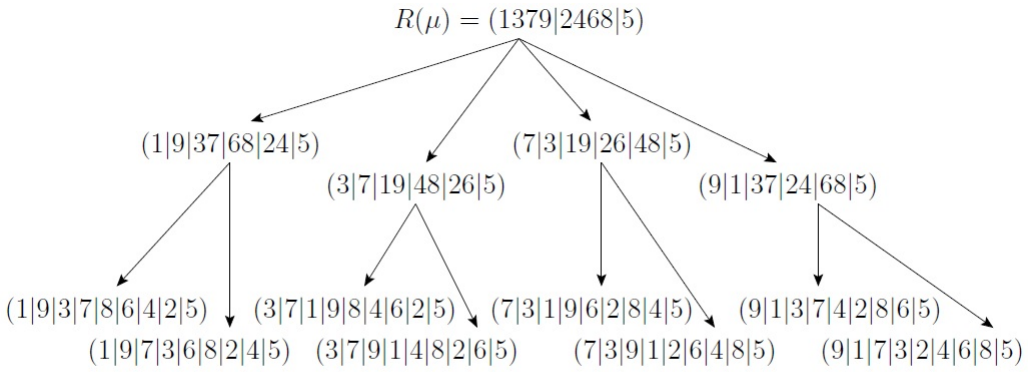

Figure A.6: Search Tree derived from the graph in picture A.5

The, considering automorphism and invariants the Tree is pruned and the resulting is the following (actually the pruning process is contemporaneous to the Refinement Function):

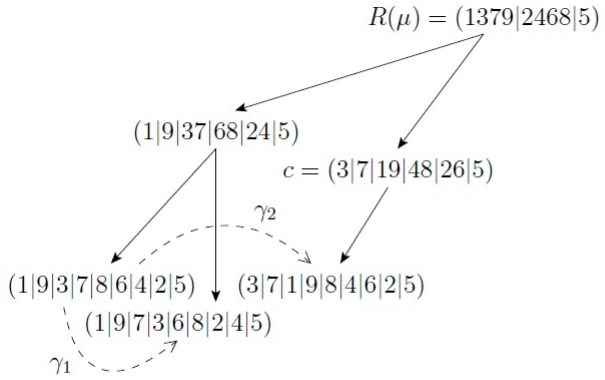

Figure A.7: The Graph derived from the graph in picture A.5 after the pruning process.

The Canonical Label in this case is the leaf(1|9|3|7|8|6|4|2|5). Then every further graphs, whose Search Tree presents a leaf like that, will be considered an isomorphic of the graph showed in ex-

ample. The corresponding Graph is the one in figure A.8:

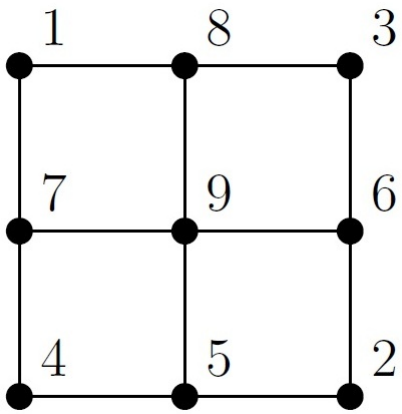

Figure A.8: The Canonical Label $L_M(G)$ of the graph G in figure A.5.

The subgraph in the figure A.8 become the label of its class and its isomorphics will be found comparing the corresponding Search Trees.

Bibliography

[1] C. R. Newey, C. Wong, Z. Irene Wang, X. Chen, G. Wu, and A. V. Alexopoulos. Optimizing spect siscom analysis to localize seizure-onset zone by using varying z scores. *Epilepsia*, 54(5):793–800, 2013.

[2] F. Wendling, F. Bartolomei, and L. Senhadji. Spatial analysis of intracerebral electroencephalographic signals in the time and frequency domain: identification of epileptogenic networks in partial epilepsy. *Philosophical Transactions of the Royal Society A: Mathematical, Physical and Engineering Sciences*, 367(1887):297–316, 2009.

[3] J. Bourien, F. Bartolomei, J. J. Bellanger, M. Gavaret, P. Chauvel, and F. Wendling. A method to identify reproducible subsets of co-activated structures during interictal spikes. application to intracerebral eeg in temporal lobe epilepsy. *Clinical neurophysiology*, 116(2):443–455, 2005.

[4] F. Bartolomei, P. Chauvel, and F. Wendling. Epileptogenicity of brain structures in human temporal lobe epilepsy: a quantified study from intracerebral eeg. *Brain*, 131(7):1818–1830, 2008.

[5] P. van Mierlo, E. Carrette, H. Hallez, K. Vonck, D. Van Roost, P. Boon, and S. Staelens. Accurate epileptogenic focus localization through time-variant functional connectivity analysis

of intracranial electroencephalographic signals. *NeuroImage*, 56(3):1122–1133, 2011.

[6] R. S. Fisher, W. Boas, W. Blume, C. Elger, P. Genton, P. Lee, and J. Engel. Epileptic seizures and epilepsy: definitions proposed by the international league against epilepsy (ilae) and the international bureau for epilepsy (ibe). *Epilepsia*, 46(4):470–472, 2005.

[7] W. A. Hauser et al. Status epilepticus: frequency, etiology, and neurological sequelae. *Advances in neurology*, 34:3, 1983.

[8] N. J. Hanna, M. Black, J. W. Sander, W. H. Smithson, R. Appleton, S. Brown, and D. R. Fish. National sentinel clinical audit of epilepsy-related death: report 2002. epilepsy-death in the shadows. 2002.

[9] T. S. Walczak, I. E. Leppik, M. D'amelio, J. Rarick, E. So, P. Ahman, K. Ruggles, G. D. Cascino, J. F. Annegers, and W. A. Hauser. Incidence and risk factors in sudden unexpected death in epilepsy a prospective cohort study. *Neurology*, 56(4):519–525, 2001.

[10] J. Engel, T. A Pedley, and J. Aicardi. *Epilepsy: a comprehensive textbook*, volume 1. Lippincott Williams & Wilkins, 2008.

[11] D. C. Taylor, M. A. Falconer, C. J. Bruton, and J. A. N. Corsellis. Focal dysplasia of the cerebral cortex in epilepsy. *Journal of Neurology, Neurosurgery & Psychiatry*, 34(4):369–387, 1971.

[12] A. Palmini, I. Najm, G. Avanzini, T. Babb, R. Guerrini, N. Foldvary-Schaefer, G. Jackson, H. O. Lüders, R. Prayson, and R. Spreafico. Terminology and classification of the cortical dysplasias. *Neurology*, 62(6 suppl 3):S2–S8, 2004.

[13] V. Y. Wang, E. F. Chang, and N. M. Barbaro. Focal cortical dysplasia: a review of pathological features, genetics, and surgical outcome. *Neurosurgical Focus*, 20(1):1–7, 2006.

[14] R. Guerrini, W. B. Dobyns, and A. J. Barkovich. Abnormal development of the human cerebral cortex: genetics, functional consequences and treatment options. *Trends in neurosciences*, 31(3):154–162, 2008.

[15] C. A. Pagni and F. Zenga. Posttraumatic epilepsy with special emphasis on prophylaxis and prevention. In *Re-Engineering of the Damaged Brain and Spinal Cord*, pages 27–34. Springer, 2005.

[16] A. E Walker. Post-traumatic epilepsy. *Textbook of Traumatic Brain Injury*, page 265, 2011.

[17] J. C. Sackellares. Long-term monitoring in epilepsy. *Journal of Clinical Neurophysiology*, 4(4):417–418, 1987.

[18] G. H. Barnett, R. C. Burgess, G. J. Skipper, C. R. Edwards, and H. Luders. Epidural peg electrodes for the presurgical evaluation of intractable epilepsy. *Neurosurgery*, 27(1):113–115, 1990.

[19] A. R. Wyler, G. A. Ojemann, E. Lettich, and A. A. Ward Jr. Subdural strip electrodes for localizing epileptogenic foci. *Journal of neurosurgery*, 60(6):1195–1200, 1984.

[20] J. Talairach and C. Fontaine. *Approche nouvelle de la neurochirurgie de l'épilepsie: méthodologie stéréotaxique et résultats thérapeutiques*. Masson, 1974.

[21] R. Mai and F. Cardinale. Robotic implantation of intracerebral electrodes in epilepsy surgery. *Neurosurgery and robotics*, 12:24, 2011.

[22] P. Kahane, E. Landré, L. Minotti, S. Francione, and P. Ryvlin. The bancaud and talairach view on the epileptogenic zone: a working hypothesis. *Epileptic disorders*, 8:S16, 2006.

[23] F. Cardinale, M. Cossu, L. Castana, G. Casaceli, M. P. Schiariti, A. Miserocchi, D. Fuschillo, A. Moscato, C. Caborni, and G. Arnulfo. Stereoelectroencephalography: Surgical methodology, safety, and stereotactic application accuracy in 500 procedures. *Neurosurgery*, 72(3):353–366, 2013.

[24] C. Munari and J. Bancaud. The role of stereo-electroencephalography (seeg) in the evaluation of partial epileptic patients. *The epilepsies. London: Butterworths*, pages 267–306, 1987.

[25] W. T. Kerr, S. T. Nguyen, A. Y. Cho, E. P. Lau, D. H. Silverman, P. K. Douglas, N. M. Reddy, A. Anderson, J. Bramen, and N. Salamon. Computer-aided diagnosis and localization of lateralized temporal lobe epilepsy using interictal fdg-pet. *Frontiers in neurology*, 4, 2013.

[26] H. Damen, D. Henneberg, and B. Weimann. Siscom - a new library search system for mass spectra. *Analytica Chimica Acta*, 103(4):289–302, 1978.

[27] J. Engel Jr. *Seizures and epilepsy*, volume 83. OUP USA, 2013.

[28] F. Wendling, J. Bellanger, F. Bartolomei, and P. Chauvel. Relevance of nonlinear lumped-parameter models in the analysis of depth-eeg epileptic signals. *Biological cybernetics*, 83(4):367–378, 2000.

[29] F. Wendling, F. Bartolomei, J.J. Bellanger, and P. Chauvel. Interpretation of interdependencies in epileptic signals using a macroscopic physiological model of the eeg. *Clinical neurophysiology*, 112(7):1201–1218, 2001.

[30] J. Bourien, J. Bellanger, F. Bartolomei, P. Chauvel, and F. Wendling. Mining reproducible activation patterns in epileptic intracerebral eeg signals: application to interictal activity. *Biomedical Engineering, IEEE Transactions on*, 51(2):304–315, 2004.

[31] M. W. Brown III, B. E. Porter, D. J. Dlugos, J. Keating, A. B. Gardner, P. B. Storm Jr, and E. D. Marsh. Comparison of novel computer detectors and human performance for spike detection in intracranial eeg. *Clinical neurophysiology*, 118(8):1744–1752, 2007.

[32] G. Varotto, S. Franceschetti, R. Spreafico, L. Tassi, and F. Panzica. Partial directed coherence estimated on stereo-eeg signals in patients with taylor's type focal cortical dysplasia. In *Engineering in Medicine and Biology Society (EMBC), 2010 Annual International Conference of the IEEE*, pages 4646–4649. IEEE, 2010.

[33] G. Varotto, L. Tassi, S. Franceschetti, R. Spreafico, and F. Panzica. Epileptogenic networks of type ii focal cortical dysplasia: A stereo-eeg study. *Neuroimage*, 2012.

[34] F. L. Da Silva, J. P. Pijn, and P. Boeijinga. Interdependence of eeg signals: linear vs. nonlinear associations and the significance of time delays and phase shifts. *Brain Topography*, 2(1-2):9–18, 1989.

[35] S. S Shen-Orr, R. Milo, S. Mangan, and U. Alon. Network motifs in the transcriptional regulation network of escherichia coli. *Nature genetics*, 31(1):64–68, 2002.

[36] R. Milo, S. Shen-Orr, S. Itzkovitz, N. Kashtan, D. Chklovskii, and U. Alon. Network motifs: simple building blocks of complex networks. *Science Signaling*, 298(5594):824, 2002.

[37] S. Wernicke. Efficient detection of network motifs. *Computational Biology and Bioinformatics, IEEE/ACM Transactions on*, 3(4):347–359, 2006.

[38] B. D. McKay. *Practical graph isomorphism.* Department of Computer Science, Vanderbilt University, 1981.

[39] B. D. McKay. Nauty user's guide (version 2.4). *Computer Science Dept., Australian National University*, 2007.

[40] B. D. McKay and A. Piperno. Practical graph isomorphism, ii. *arXiv preprint arXiv:1301.1493*, 2013.

[41] S. Wernicke and F. Rasche. Fanmod: a tool for fast network motif detection. *Bioinformatics*, 22(9):1152–1153, 2006.

[42] B. J. Frey and D. Dueck. Clustering by passing messages between data points. *science*, 315(5814):972–976, 2007.

[43] G. D. Cascino. Surgical treatment for extratemporal epilepsy. *Current treatment options in neurology*, 6(3):257–262, 2004.

[44] S. G. Hartke and A. J. Radcliffe. Mckay's canonical graph labeling algorithm. *Communicating Mathematics*, 479:99–111, 2009.